UNIVERSITÉ DU QUÉBEC

MÉMOIRE

PRÉSENTÉ À

L'UNIVERSITÉ DU QUÉBEC À CHICOUTIMI

COMME EXIGENCE PARTIELLE

DE LA MAÎTRISE EN SCIENCES APPLIQUÉES

PAR

SIMON MATTE

ANALYSE DE LA VALEUR ÉCONOMIQUE D'UN SYSTÈME DE PRÉVISION PROBABILISTE DES INONDATIONS : CAS DE LA RIVIÈRE MONTMORENCY

MARS 2017

Résumé

Prévoir et se préparer aux inondations représente un enjeu majeur au Québec. Pour y parvenir, la Direction de l'Expertise Hydrique du Québec fait équipe avec les municipalités de la province afin de détecter les risques de cet aléa aussi tôt et fidèlement que possible et d'engager des mesures d'urgences. Cependant, il existe une multitude de méthodes permettant de modéliser le comportement futur d'un cours d'eau et de transmettre l'incertitude sur cette prévision aux autorités concernées.

L'objectif de ce projet de maitrise se divise en deux parties. Premièrement, de comparer différentes approches de modélisation hydrologique en faisant varier l'intrant météorologique et en tenant compte de l'incertitude sur l'état de départ d'un bassin versant. Deuxièmement, de construire une plateforme de comparaison des performances basée sur l'analyse de la valeur économique de chaque système dans un contexte de prévention et de préparation aux inondations.

Le projet compare trois systèmes de prévisions hydrologiques probabilistes sur la rivière Montmorency (incluant une reproduction du système en place), pour la période 2011-2014. Chaque système passe ensuite par un décideur artificiel devant engager des dépenses préventives dans le but de réduire les dégâts potentiels (matériels et psychologiques) des inondations futures. La valeur de chaque système est comparée en tenant compte du niveau d'aversion au risque de l'utilisateur et de la valeur accordée aux dommages intangibles des inondations.

Ce mémoire conclue en cernant les critères de conception d'un système de prévision ayant le plus gros impact sur la valeur opérationnelle du système, permettant d'aller au-delà des outils de mesure de performance statistique conventionnels (CRPS, fiabilité, LOG score). Enfin, il souligne des pistes de projets futurs s'appuyant sur les conclusions tirées.

Remerciements

La section remerciements : une toute petite section informelle d'un long document sérieux se donnant le droit d'adresser directement le lecteur, révélant par le fait même une facette de la personnalité de l'auteur. Forme justifiée, de mon opinion, puisqu'un discours informel laisse transparaitre la sincérité de l'auteur. C'est donc modestement, mais surtout, sincèrement, que j'exprime les remercîments suivants :

Merci à ma directrice Marie-Amélie Boucher d'avoir prodigué autant de support et d'intérêt dans le projet (c'était son idée, après tout…). Plus sérieusement, la réussite du projet de recherche aurait été impossible sans sa réserve infinie d'énergie.

Merci à Vincent Boucher, Thomas-Charles Fortier Filion et Michel Leclerc pour leur disponibilité et leur participation. Ils ont été des ressources et des experts indispensables permettant de joindre les parties multidisciplinaires du projet.

Plus localement, merci aux membres du groupe R2Eau. Mine de rien, avoir une appartenance à un groupe d'étudiant et de professeurs qui partagent les mêmes domaines de recherche joue pour beaucoup dans la motivation d'un étudiant à accomplir son projet. Salutations particulières à Romain, qui, démarrant régulièrement le tour de table hebdomadaire par moi, me forçait à inventer rapidement quelque chose pour cacher qu'en fait, je n'avais rien accompli de la semaine.

Coucou à Geneviève, Ève et Yasmine, pour l'expérience inoubliable d'une baignade dans la rivière Caribou qui a couté cher.

Pour terminer, merci à l'un de mes meilleurs amis Guillaume, pour m'avoir accompagné dans mes périodes de procrastination et m'avoir répété la question interdite un nombre incalculable de fois : « Pis, tu finis quand ta maîtrise? ».

Table des matières

Liste des figures

Liste des tableaux

1. Introduction

1.1 Problématique générale

L'eau douce est l'une des ressources les plus abondantes au Québec, recouvrant 22% de sa superficie répartie en près de 3,6 millions de plans d'eau et des dizaines de milliers de ruisseaux de rivières donc le réseau totalise plusieurs millions de kilomètres (Gouvernement du Québec, 2014). Cette particularité de la province offre un potentiel énorme en termes d'aménagements municipal, de production d'hydroélectricité et de récréation. Cependant, cette situation rend également vulnérable la population riveraine aux aléas naturels tels que les inondations, en faisant la catastrophe naturelle la plus fréquente de la province (Gouvernement du Québec, 2014).

Depuis 1990, on dénombre 27 inondations de niveau catastrophique ayant touché la population du Québec, incluant entre autres le Déluge du Saguenay (1996), ou plus récemment le débordement de la rivière Richelieu (2011). Il y a 15 ans, le Gouvernement du Québec a décidé de mettre des mesures en place afin de gérer la situation. Le ministère du Développement Durable, de l'Environnement et de la Lutte contre les Changements Climatiques (MDDELCC) fonda alors le Centre d'Expertise Hydrique du Québec (CEHQ) en 2001, en lui attribuant la mission de « gérer le régime hydrique du Québec avec une préoccupation de sécurité, d'équité et de développement durable » (lien CEHQ). Plus précisément, celui-ci veille à la régularisation et à la

surveillance des barrages publics, procure un soutien aux municipalités dans la lutte contre les inondations et approfondit les connaissances hydrologiques et hydrauliques pour assurer la gestion de l'eau. Depuis 2015, l'organisme est connu sous le nom de la Direction de l'Expertise Hydrique (DEH) suite à une réorganisation structurelle. La DEH est équipée aujourd'hui d'un réseau d'environ 230 stations hydrométriques réparties sur le territoire, et surveille en temps réel le comportement des cours d'eau du Québec.

Un autre élément important pour la gestion de l'eau du Québec provient de la « Politique Nationale de l'Eau ». Depuis 2002, cette dernière existe afin d'assurer la protection de l'eau comme ressource naturelle et d'en assurer la gestion dans une perspective de développement durable et, ce faisant, de mieux protéger la santé publique et celle des écosystèmes. Afin d'accomplir cette mission, le MDDELCC a choisi un mode de gestion territorial distribué par bassins versants, en soutenant financièrement et techniquement la mise en place de 33 « Organismes de Bassin Versant ». Ceux-ci regroupent l'ensemble des acteurs concernés par la gestion de leur eau : les municipalités, des groupes de citoyens, des entreprises privées, des agriculteurs et d'autres usagers du bassin versant. La figure suivante montre les 40 bassins surveillés et gérés par ces organismes.
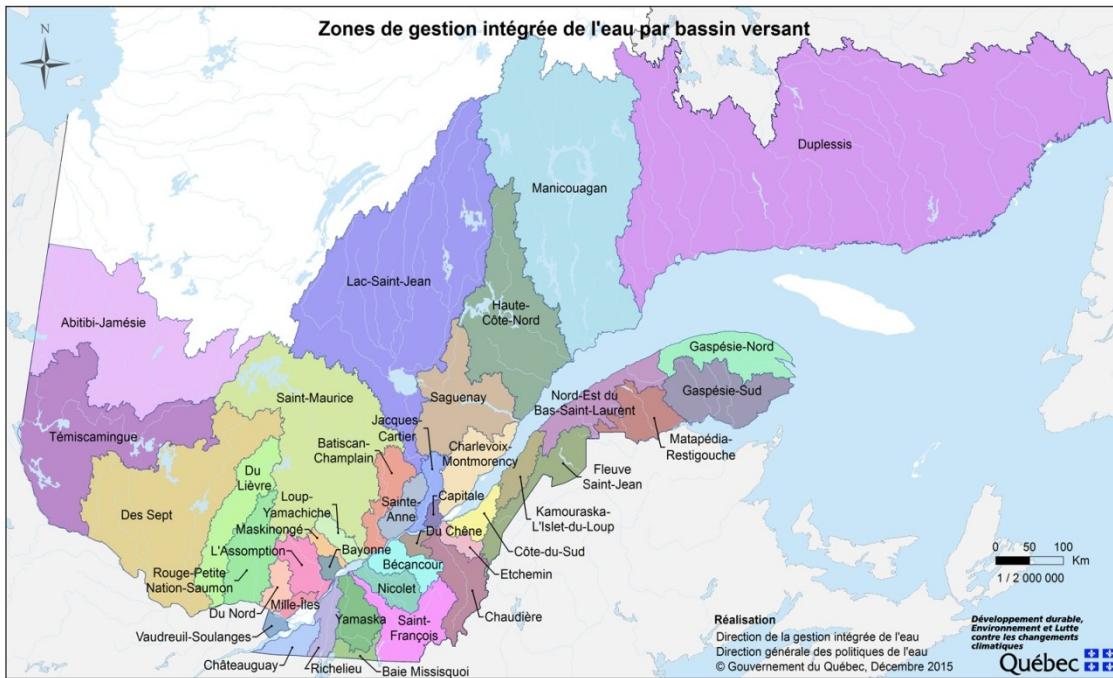
Figure 1-1 - Différentes zones de gestion intégrée de l'eau par bassin versant. Source: MDDELCC, 2015

C'est donc de concert que les municipalités, les Organismes de Bassin Versant (OBV) et la DEH travaillent afin d'assurer la sécurité de la population riveraine.

Malgré tous ces efforts, la prévention et la protection contre les inondations n'est pas une science exacte. La complexité des phénomènes en jeu ainsi que le grand nombre de paramètres déterminants font que la qualité et la fiabilité de la prévision hydrologique sont limitées par l'information disponible (bathymétrie, stations de mesures hydrologiques et météorologiques, etc.), la puissance de calcul des ordinateurs (notamment lors des simulations atmosphériques donnant une prévision météorologique), la qualité des modèles de prévision, et la disponibilité des ressources

3

(autant humaines que matérielles) pour la collecte et le traitement des données nécessaires à l'élaboration de simulations fiables et performantes. C'est pourquoi l'amélioration des prévisions hydrologiques est encore un défi d'actualité.

L'objectif du projet de recherche consiste à tenter d'établir un meilleur système de prévision hydrologique pour la rivière montmorency, dans un contexte de prévention contre les inondations. Le projet vise également à établir une base comparative permettant d'évaluer la qualité et la performance d'un système de prévision en calculant la valeur économique du système, lorsque mis à l'épreuve.

La première section de la suite du document présente donc les différents aspects du projet d'étude sur la prévision hydrologique. D'abord, le site d'étude (le bassin de la rivière Montmorency) est présenté en détails. Puis la problématique spécifique de ce secteur est expliquée, accompagnée de la présentation du système opérationnel de gestion des inondations en place actuellement. Enfin, une revue de littérature montre la théorie sur laquelle repose le cheminement intellectuel et le parcours méthodologique du projet de recherche.

Le chapitre 4 présente les résultats du projet sous la forme d'un article scientifique. Enfin, la synthèse et conclusion de l'étude sont présentées au chapitre 5.

1.2   Présentation de la zone d'étude

1.2.1   Géographie et morphologie

Le bassin versant visé par l'étude est celui de la rivière Montmorency. C'est un bassin d'une superficie de 1150 km², prenant sa source dans le lac des Neiges (dans la réserve faunique des Laurentides) et se jetant dans le fleuve St-Laurent juste en aval de la chute Montmorency, à l'est de la ville de Québec. La figure 1-2 montre l'emplacement géographique du bassin. Depuis 2011, l'OBV de Montmorency a été fusionné avec celui de la zone Charlevoix, devenant l'OBV Charlevoix-Montmorency.
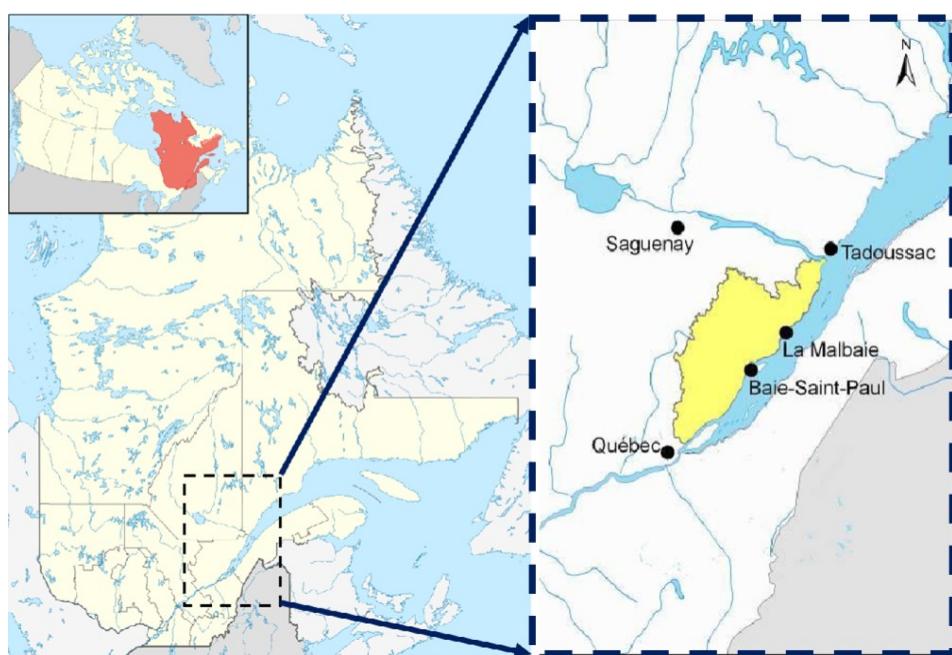
Figure 1-2 - Emplacement géographique de la zone Charlevoix-Montmorency au Québec

La figure 1-3 montre la sous-division entre le bassin versant Montmorency (visé par l'étude) à l'intérieur de la zone Charlevoix-Montmorency. L'occupation du territoire est divisée entre la section nord et sud. La partie nord du bassin est un secteur naturel forestier incluant la forêt Montmorency (la forêt d'enseignement et de recherche de l'Université Laval, totalisant 416 km²) ainsi qu'une partie de la réserve faunique des Laurentides (qui couvre 43% du bassin). Celui-ci repose sur le Bouclier Canadien, et le relief y est surtout montagneux. La partie sud est largement urbanisée. On y retrouve les municipalités de Boischatel, Beauport et Sainte-Brigitte-de-Laval, entres autres. L'agriculture y est quasi-inexistante.
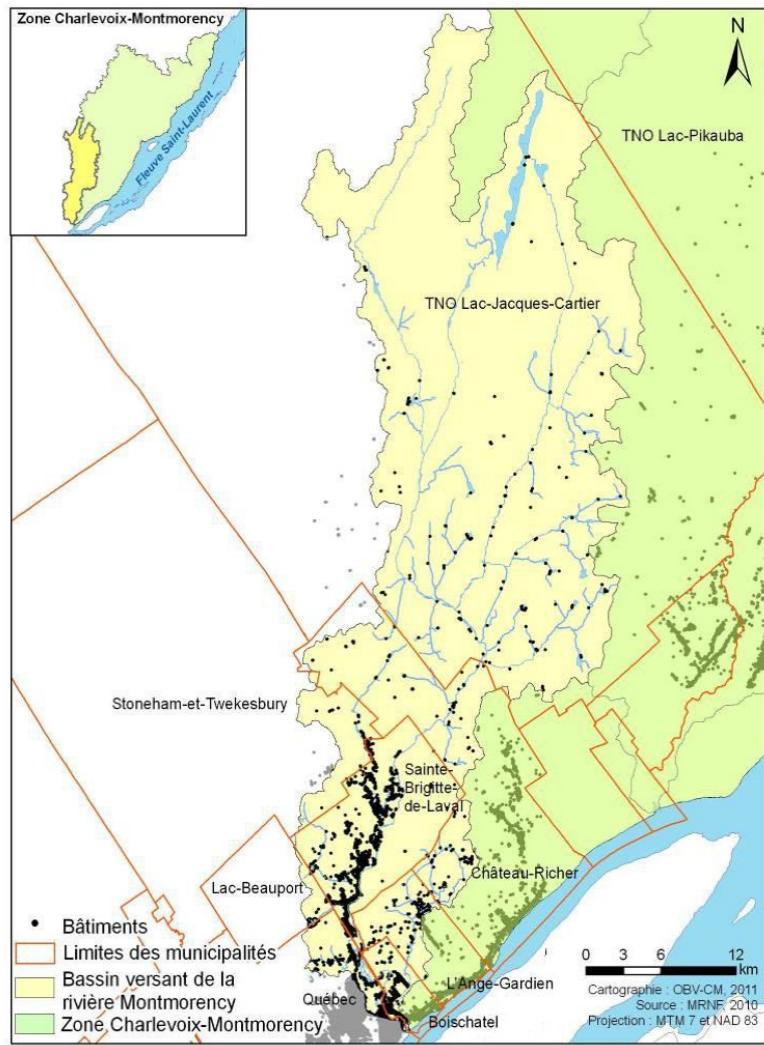
Figure 1-3 - Délimitation du sous-bassin Montmorency (en médaillon), et emplacement des aménagements urbains le long de la rivière (OBV Charlevoix-Montmorency, 2014).

La forêt recouvre 83% de la superficie du bassin. Les secteurs habités se situent majoritairement dans la ville de Québec ou le long de la partie sud de la rivière Montmorency, et totalisent près de 30 000 personnes (OBV Charlevoix-Montmorency, 2014). Le sol du sud du territoire étant riche en dépôts meubles de type fluvio-glaciaire,

une partie de la section urbanisée (sud) du bassin est occupée par l'exploitation de carrières, sablières et gravières.

La rivière Montmorency est également au centre d'un approvisionnement majeur en eau potable pour les municipalités environnantes, tel que montré à la figure 1-4. Par exemple, la ville de Québec alimente environ 150 000 résidents grâce à 2 stations de captage, desservant les arrondissements de Charlesbourg et Beauport et totalisant une demande de près de 45 000m³/jour (OBV Charlevoix-Montmorency, 2014). L'une de ces stations, appelée « Ouvrage A » a fait l'objet d'une reconstruction récente et fait partie des zones spécifiquement vulnérables aux inondations.
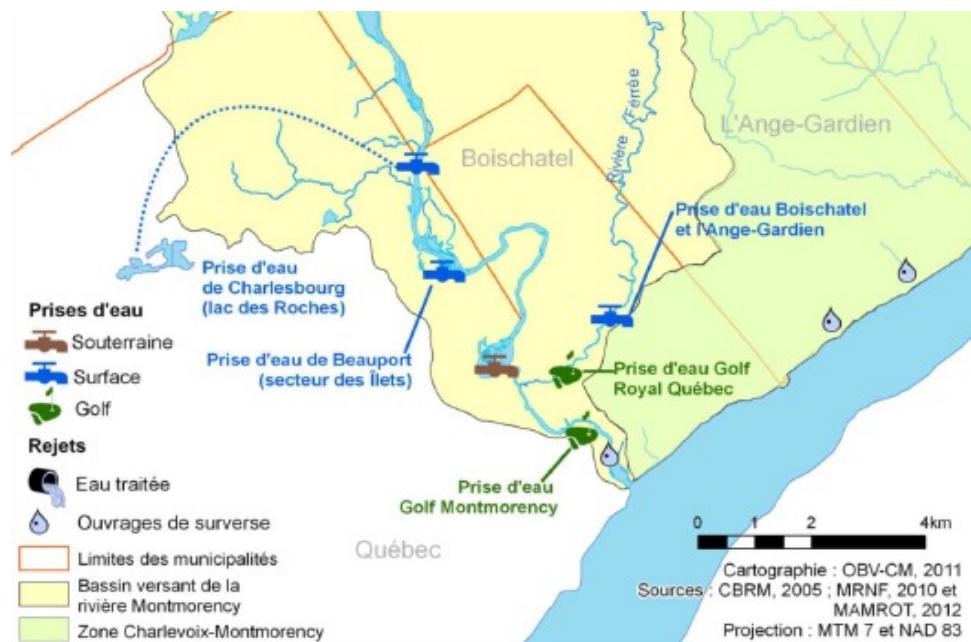
Figure 1-4 - Localisation des prises d'eau sur la rivière Montmorency (OBV Charlevoix-Montmorency, 2014)

1.2.2 Climatologie et hydrologie

Le secteur nord du bassin reçoit des précipitations parmi les plus élevées de la province. Ce sont en moyenne 1588 mm de précipitations qui s'abattent sur la région annuellement, dont 40% sous forme de neige (6,35m !). La section sud reçoit quant à elle plutôt 1230 mm en moyenne, 26% étant sous forme de neige.

La rivière Montmorency coule sur 101 km. Son débit est largement variable, allant de 35 m³/s pendant les périodes d'étiages à plus de 600 m³/s pendant les périodes de crues. Le temps de réponse du bassin est typiquement de 11 ou 12 heures. La rivière est l'objet d'une attention constante, puisqu'une partie des secteurs résidentiels de ses berges, ainsi que la station de pompage, se trouvent à l'intérieur de la zone inondable 20 ans. Les valeurs établies de débits de récurrence de la Montmorency sont montrés au tableau 1-1.

Tableau 1-1 - Périodes de retour typique des débits de la rivière Montmorency (Leclerc et al. 2001)

Récurrence	Débit [m³/s]
2 ans	439
20 ans	735
100 ans	926
Record historique (nov. 1966)	1110
1000 ans	1191

Contrairement à la pratique courante lors d'aménagement urbain à proximité des plans d'eau, la rivière Montmorency n'a pas fait l'objet d'une cartographie complète des zones inondables à l'eau libre avant 1998. Une section en particulier, le secteur des Ilets (figure 1-5) montre qu'une vingtaine de bâtiments se retrouvent à l'intérieur de la plaine inondable de récurrence 20 ans. Les propriétaires de ces résidences, dont l'installation précède la cartographique des zones inondables, ont des droits acquis sur leur terre et ont appris à vivre avec le risque constant des inondations.
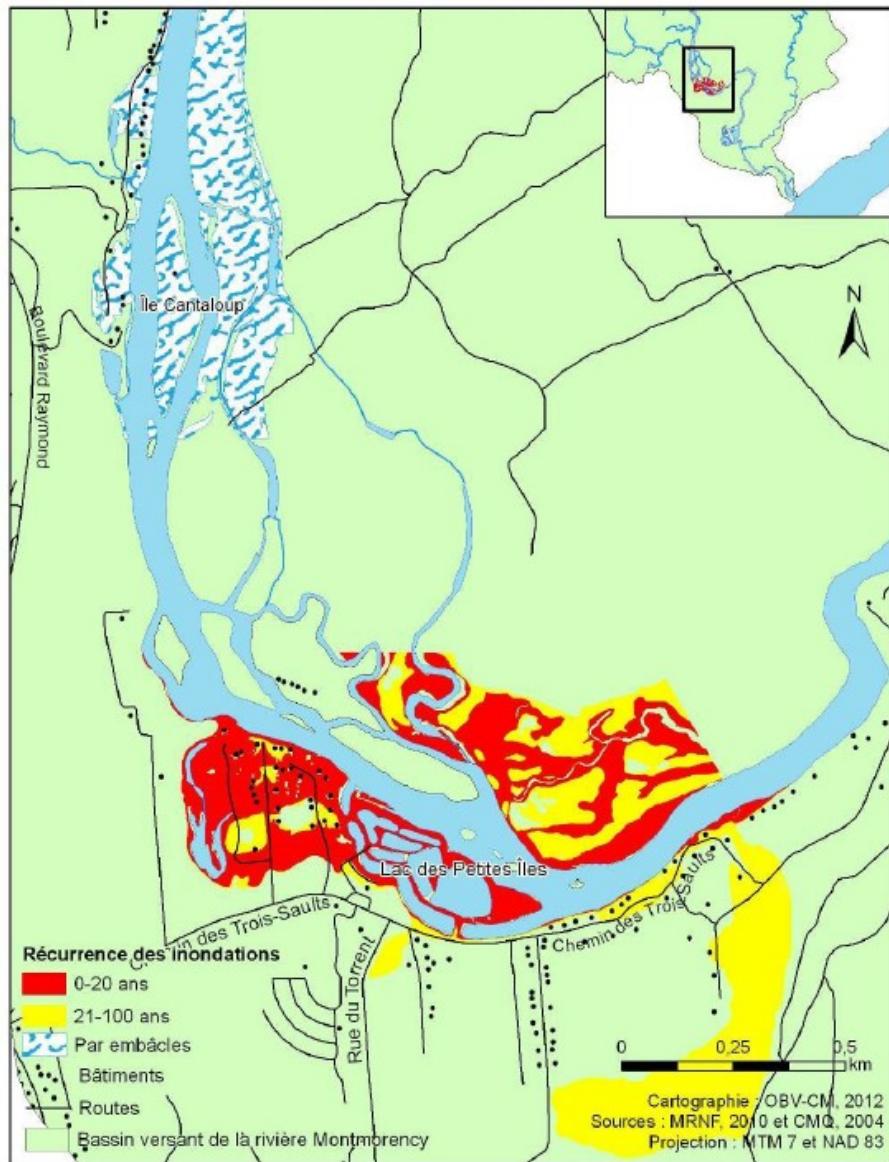
Figure 1-5 - Localisation des zones inondables du Secteur des Îlets. (Source : OBV Charlevoix-Montmorency, 2014)

Le secteur des îlets (figure 1-5) comporte une large plaine alluviale dite « secteur anastomosée ». Celle-ci consiste en une section plane où le lit de la rivière se divise en plusieurs bras parallèles. Ceux-ci servent parfois de « trop-pleins » à la rivière lors de

période de débordement. Le secteur des ilets est également une section qui suit immédiatement un tronçon de rapides. Cette particularité, en plus du coude serré que prend la rivière à cette section, font de ce secteur un endroit très propice aux embâcles de glace, qui deviennent récurrent sur une base quasi-annuelle. La combinaison de ces facteurs et de la position du site résidentiel dans la plaine inondable font du secteur des Îlets l'un des endroits les plus vulnérables et fréquemment touché par les inondations.

De plus, le passage du train de glace au moment de la débâcle peut causer des dommages importants aux berges. Pour citer quelques exemples, des températures record en mars 2012 on forcée une évacuation de 25 résidences due à la fonte accélérée des neiges. En avril 2014, une combinaison d'aléas (embâcle, débâcle et pic de fonte) a transformé une crue moyenne en un évènement semi-centenaire de par leur simultanéité, forçant une nouvelle fois l'évacuation d'un secteur. La dévalaison de la glace accumulée a causé une érosion majeure des berges et arraché deux ponceaux, tout en endommageant sévèrement un troisième.

1.3   Système de prévision opérationnel actuel

Dans l'exercice de ses fonctions, la DEH emploie les données météorologiques du DSEE (Direction du Suivi de l'État de l'Environnement), les données hydrométriques recueillies sur le terrain, les prévisions météorologiques d'ECCC (Environnement et Changements Climatiques Canada) et le modèle hydrologique HYDROTEL (Fortin et al.,

1995). Ces informations, ainsi que les observations récentes de débit, de niveau et de neige, leur permettent d'émettre des prévisions de débit en continu sur les rivières les plus à risque du Québec. Les prévisions sont émises jusqu'à un horizon de 5 jours selon un pas de temps de 3h, et disponibles sur internet[1], autant pour le grand public que pour les intervenants locaux. Afin d'offrir une mesure de l'incertitude sur la prévision, le CEHQ « habille » la courbe prévisionnelle d'une enveloppe d'incertitude d'un niveau de confiance 50%. Ce modèle d'habillage statistique a été développé par Huard (2013) et représente « les erreurs prévisionnelles passées associées à un maximum de 10 années d'historique de prévision [opérationnelles, obtenues depuis la simulation de la prévision météo déterministe] » (Huard 2013).

Responsable de la gestion du bassin Montmorency, le bureau de la sécurité publique de la ville de Québec est l'un des intervenants utilisant la prévision hydrologique émise par la DEH. Celui-ci analyse l'information recueillie et a le rôle de prendre la décision d'engager ou non des mesures de sécurité visant à protéger la population d'une inondation imminente probable. Pour s'aider dans cette tâche, la ville de Québec a préétablie des « seuils de dépassement » permettant de lancer des mesures

[1] http://www.cehq.gouv.qc.ca/prevision/index.asp

incrémentales d'actions, jusqu'à l'évacuation d'urgence. Ceux-ci sont montrés au tableau 1-2 et ont été fixé par une étude de Leclerc et al. (2012).

Tableau 1-2 - Seuils de dépassement pour le secteur résidentiel des Ilets (Rigolet)

Débit prévu à la station (CEHQ #051001) [m³/s]	Niveau d'alerte	Mesures d'actions
350	Veille	Avertissement dans les services que les niveaux d'eau sont hauts
450	Pré-alerte	Mobilisation des effectifs
500	Alerte	Mise en place de mesures de protections
550	Inondation	Évacuation active

2. REVUE DE LITTÉRATURE

2.1   L'utilité de la prévision d'ensemble en hydrologie

La prévision hydrologique est une science incertaine. Par conséquent, afin de représenter le plus fidèlement possible la réalité stochastique de ce domaine, il est justifiable d'accompagner une prévision donnée d'une mesure d'incertitude. Pour parvenir à ce résultat, il existe plusieurs manières de procéder. La méthode de la DEH s'apparente à un système « habillé », ou l'erreur sur la prévision est estimée en moyennant les erreurs prévisionnelles passées dans des conditions semblables (Huard, 2013). Cette méthode est en application chez plusieurs agences opérationnelles (ex. Hamill and Whitaker, 2006; Diomede et al., 2008; Marty et al., 2012).

Il est aussi possible de simuler plusieurs « scénarios », chacun reposant sur des méthodes ou des hypothèses différentes (comme en variant le modèle hydrologique, ou en introduisant des prévisions météos probabilistes, etc.), et de rassembler ces résultats sous la forme d'un ensemble prédictif où chaque scénario a une probabilité de se réaliser. C'est-ce qu'on appelle la prévision d'ensemble.

La communauté scientifique est généralement en accord sur le fait que les prévisions d'ensemble ont une valeur supérieure à la prévision déterministe (Jaun et al., 2008; Velazquez et al., 2010; He et al., 2013, et plusieurs autres). Cette preuve a aussi

été faite (ex. Roulin, 2007; Velazquez et al., 2009; Boucher et al. 2012) grâce à plusieurs outils statistiques, comme des mesures telles que le Continuous Ranked Probability Score (CRPS, Gneiting et Raftery, 2007) et le score de Brier (Brier, 1950).

Toutefois, pour être qualifiée de *bonne*, une prévision ne se doit pas que d'être juste. Pour être *utile*, elle se doit, lorsqu'elle est utilisée dans un contexte de réduction des impacts d'une inondation, de permettre de réaliser des économies. C'est ce qu'on appelle la *valeur* (Murphy, 1993).

2.2 La valeur économique de la prévision et l'aversion au risque

Estimer l'impact économique d'une prévision n'est pas proprement nouveau. Dans le cas de la production d'hydroélectricité, la valeur d'un système de prévision est facilement interprétable en terme d'énergie produite, et a déjà fait l'objet de recherches (ex : Boucher et al., 2012; Carpentier et al., 2013; Côte and Leconte, 2016). L'approche pour la détermination de la valeur d'un système de prévention d'inondation est totalement différente. Généralement, celle-ci est estimée grâce à une comparaison des dépenses (mesures de protection) et dégâts (inondation) selon le modèle « coutspertes » ou $\mathrm{Cost/Loss}$ ratio (e.x. Murphy, 1977; Richardson, 2000; Roulin, 2007; Verkade and Werner, 2011; Abaza et al., 2014)

Toutefois, cette méthode n'est pas sans lacunes. Elle n'exploite pas toute l'information contenue dans une prévision probabiliste. Elle ne tient pas en compte de

16

la nature humaine du processus de décision, qui va être influencée par une aversion (généralement) au risque de l'utilisateur. Afin de palier à ces manques, le projet actuel emprunte à une discipline bien familière avec l'évaluation de la valeur d'une décision basé sur des probabilités et des risques : l'économie.

La détermination de la valeur d'un système de prévision passera par la fonction d'utilité de von Neumann and Morgenstern (von Neumann and Morgenstern, 1944), qui reflète la préférence de l'utilisateur face à l'incertitude (risquophobe, neutre ou risquophile). Les détails méthodologiques sont expliqués dans la section suivante, présentant l'article.

3. Méthodologie générale

La figure 3-1 présente l'organisation et la méthodologie du processus de traitement de données pour arriver aux prévisions hydrologiques finales. D'abord, les données météorologiques *observées* sont simulées dans HYDROTEL. Le débit simulé obtenu est comparé au débit observé pour la même période. Naturellement, la correspondance de ces deux derniers n'est pas parfaite, du à plusieurs raisons. Pour n'en citer que quelques-unes, il existe :

- l'erreur d'observation météo (sous-captation des précipitations ou distribution insuffisante de stations météos sur le bassin) ;

- la qualité de la calibration du modèle hydrologique (faite dans une optique de maximiser la performance du modèle sur une longue chronique, mais où certaines périodes sont moins bien représentées que d'autres) et;

- la nature du modèle hydrologique lui-même (hypothèses simplificatrices, choix des sous-modèles, etc.).
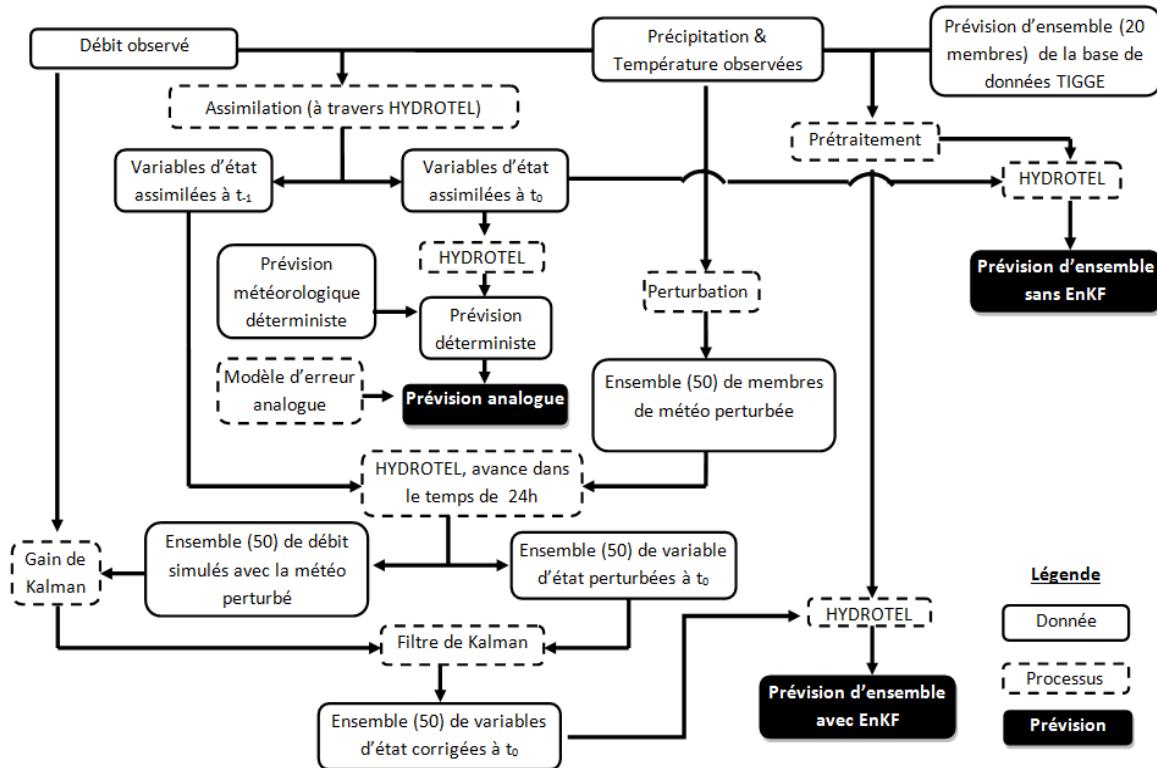
Figure 3-1- Organigramme de la procédure de production des prévisions hydrologiques

Afin d'émettre des prévisions à partir d'une simulation, il est nécessaire de d'abord ramener l'état simulé du bassin vers la meilleure estimation possible des conditions réelles de celui-ci. À cette fin, des relevés manuels de neige sont fait périodiquement sur le terrain de façon à corriger l'épaisseur du couvert neigeux de la simulation. Cependant, il n'est simplement pas réaliste d'instrumenter l'intégralité du bassin afin de mesurer en continu l'humidité du sol, l'équivalent en eau de la neige, et l'écoulement de surface. Par conséquent, on s'en remet à l'expertise hydrologique du prévisionniste pour juger des corrections à apporter aux variables d'état. Dans le cas d'HYDROTEL, cette correction est effectuée indirectement en apportant itérativement des

19

modifications manuelles sur les précipitations (amplitude des crues dues à la pluie), températures (synchronisation des évènements de fonte de neige), niveaux de neige et contenu en eau du sol afin que la simulation reproduise la série des débits observés. Ce processus s'appelle *assimilation de données manuelle*, et les résultats sont montrés dans la section suivante. Un exemple détaillé décrivant une démarche semblable peut être vu dans le mémoire de maîtrise de Mamono, 2010.

Par la suite, les variables d'état du bassin sont sauvegardées à tous les pas de temps. Celles-ci représentent, au meilleur des connaissances disponibles, l'estimation des conditions du bassin (neige, humidité du sol, écoulement en surface et en rivière) pour toute la période d'étude. On peut donc reprendre (charger) les conditions à un temps de simulation t_0 (« instant présent ») et lancer une prévision à partir de ce point. Pour la prévision dite « habillée », la prévision météo déterministe est entrée dans HYDROTEL, afin de produire une prévision hydrologique unique. On y applique un modèle d'habillage conçu par Huard (2013), représentant la moyenne des erreurs de prévisions sur un historique de 10 années sur 11 rivières du Québec, répartie en 50 quantiles et tenant compte de la saisonnalité et de l'horizon de prévision.

En habillant la prévision déterministe de ce modèle d'erreur, on obtient la prévision « contrôle », que le projet de recherche actuel reconstruit comme base comparative.

Pour les prévisions d'ensemble, la démarche varie. D'abord, les prévisions météorologiques TIGGE[2] sont comparées aux valeurs observées, afin de détecter et corriger un biais systématique. Ensuite, les données météos dé-biaisées sont passées directement dans HYDROTEL avec les états assimilés à t_0, afin de produire le premier système de prévision d'ensemble : « Prévision d'ensemble sans filtre d'ensemble de Kalman (EnKF) » (Evensen, 2003). Cependant, ce système de prévision présente un problème majeur de performance : la fiabilité de la prévision à court-terme (24h). Puisque la source d'incertitude ne provient que la dispersion des membres météo, c'est l'état initial (unique) du bassin qui domine le résultat du début de la simulation hydrologique. Pendant les premiers pas de temps de simulation, tous les membres sont pratiquement identiques et ne se séparent qu'une fois que le temps de réponse du bassin (12h) permet une dispersion de la réponse des différents scénarios météo. Pour remédier à ce problème, un outil mathématique fut utilisé : le filtre d'ensemble de Kalman (*Ensemble Kalman Filter*, EnKF).

---

[2] *The Observing System Research and Predictability Experiment Interactive Grand Global Ensemble* : une banque de données mondiales accessibles à tous recensant les prévisions hydrologiques faite historiquement par les grands centres sur la planète.

3.1 Le filtre d'ensemble de Kalman

Le filtre d'ensemble de Kalman (EnKF) est un outil mathématique permettant, dans son application, de poser une meilleure estimation de l'état d'un système en combinant simultanément l'information sur l'observation de l'état du système et la prévision préalablement faite sur celui-ci. Le cas d'application en hydrologie n'est pas nouveau, et la démarche offerte par Abaza et al. (2015) a été utilisée. Le processus est relativement complexe et sera détaillé entièrement dans le mémoire de maîtrise. Tout d'abord, les variables d'état sauvegardées 24h avant « l'instant présent » (donc, t_{-1}) sont reprises. Puis, des bornes de perturbations sont établies. Puisque dans la méthode actuelle d'HYDROTEL, l'ajustement des variables d'état se fait par l'intermédiaire de la météo observée, c'est cette dernière qui sera perturbée. Les bornes en question sont montrées au tableau 3-1. Un ensemble de 50 scénarios de météo perturbées est créé. Chacun de ces scénarios est ensuite simulé dans HYDROTEL entre l'instant t_{-1} et t_0 (24h), afin de permettre au bassin modélisé de répondre aux différentes conditions météo. Celui-ci nous retourne le résultat (50 débits perturbés correspondant) et le nouvel état du bassin (50 groupes d'états).

Tableau 3-1 - Bornes de perturbation de la météo observée dans l'application du filtre d'ensemble de Kalman

	Température [°C]	Précipitation (facteur mutiplicatif)	Précipitation (facteur additif [mm/3h])
Borne supérieure	+8	X 1.5	+0.5
Borne inférieure	-8	X0.5	0

Puis, le débit réel observé à t_0 est également perturbé, selon une distribution normale (en pigeant 50 valeurs). Cette perturbation permet d'abord de représenter qu'il existe une incertitude sur les mesures de débit, et de permettre une certaine dispersion de la réponse à l'étape suivante[3].

Un à un, l'EnKF évalue la « performance » de chacun des scénarios en comparant le débit de la simulation perturbée avec un débit pigé au hasard depuis la distribution normale. Lorsque les deux correspondent bien, le filtre juge que le scénario est bon et accorde une forte confiance à celui-ci (c'est la valeur du *gain de Kalman*). Lorsque les

[3] Sans cette dispersion, tous les états se feraient « ramener » trop fortement vers l'état de référence, et l'utilité du filtre (obtenir une certaine dispersion des points de départ de simulation) en serait réduite.

deux sont très différents, le filtre juge que le scénario est improbable, et lui accorde une confiance fiable.

La valeur du gain de Kalman sert ensuite de pondération dans le calcul d'un juste milieu entre les états perturbés et la valeur estimée réelle – inconnue – du bassin. Par conséquent, c'est la *moyenne* de tous les scénarios perturbés qui est utilisée comme référence[4], ce qui revient au même que l'état assimilé du bassin à t_0. Un scénario au gain de Kalman élevé verra ses états pratiquement inchangés, alors qu'un scénario au gain plus faible se verra « ramené » partiellement vers les valeurs de référence.

Le résultat est en ensemble (50) de variables d'états à t_0, toutes légèrement différentes, mais grossièrement centrées et rapprochées vers la simulation initiale de référence (obtenue par le processus d'assimilation manuelle).

---

[4] Bien qu'il aurait été en effet plus simple de comparer directement à l'état de référence t_0, celui-ci n'est pas toujours connu, dépendamment du contexte dans lequel le filtre de Kalman est appliqué. Afin de rester fidèle aux démarches fournies par Abaza et al. (2015), la moyenne des états perturbés fut utilisée comme référence.

Enfin, l'une des particularités de l'EnKF qui n'a pas encore été mentionnée est qu'il permet d'admettre que différentes combinaisons de variables d'état peuvent donner des réponses équivalentes. Lors du processus d'assimilation manuelle, une unique solution à l'état du bassin doit être fixée. Par contre, l'EnKF peut détecter d'autres combinaisons d'états simulant le débit observé à t_0. En d'autres mots, ceci permet avantageusement d'inclure une incertitude sur l'état du bassin dans la simulation, puisque bien que ces scénarios se comportent semblablement à t_0, leur réponse face à la météo future peut varier.

Pour terminer, en combinant les 20 scénarios météos aux 50 scénarios d'état du bassin, on obtient la « prévision d'ensemble avec EnKF ». Afin d'alléger la tâche de calcul, chacun des 20 membres météo fut attribué aléatoirement (avec remise) à l'un des scénarios d'état, permettant de réduire la charge de simulation de 1000 combinaisons à 50. Il a été démontré que cette méthode ne réduit pas significativement la qualité des prévisions (Abaza et al., 2015).

Le chapitre suivant est un article scientifique qui a été soumis dans *Hydrology and Earth System Sciences* le 21 septembre 2016, Il reprend la mise en contexte et la méthodologie présentées dans les chapitres précédant et actuel. Il présente aussi les principaux résultats et conclusions. Quelques figures de résultats supplémentaires ont été omises de l'article et sont présentées l'annexe A.

Chapter 4

Moving beyond the cost-loss ratio: Economic assessment of streamflow forecasts for a risk-averse decision maker

[1] Simon Matte

[1] Marie-Amélie Boucher

[2] Vincent Boucher

[3] Thomas-Charles Fortier Filion

[1] Dept. of Applied Sciences, Université du Québec à Chicoutimi, 555, boulevard de l'Université, Chicoutimi, G7H 2B1, Canada

[2] Dept. of Economics, Université Laval, 1025, avenue des Sciences-Humaines, Québec, G1V 0A6, Canada

[3] Québec Government Direction of Hydrologic Expertise, 675, boul. René Lévesque Est., Québec, G1R 5V7, Canada

Correspondence to Marie-Amélie Boucher (marie-amelie_boucher@uqac.ca)

4.1 Abstract

A large effort has been made over the past 10 years to promote the operational use of probabilistic or ensemble streamflow forecasts. Numerous studies have shown that ensemble forecasts are of higher quality than deterministic ones. Many studies also conclude that decisions based on ensemble rather than deterministic forecasts lead to better decisions in the context of flood mitigation. Hence, it is believed that ensemble forecasts possess a greater economic and social value for both decision makers and the general population. However, the vast majority, if not all, of existing hydro-economic studies rely on a cost-loss ratio framework that assumes a risk-neutral decision maker. To overcome this important flaw, this study borrows from economics and evaluates the economic value of early warning flood systems using the well-known Constant Absolute Risk Aversion (CARA) utility function, which explicitly accounts for the level of risk aversion of the decision maker. This new framework allows for the full exploitation of the information related to a forecasts' uncertainty, making it especially suited for the economic assessment of ensemble or probabilistic forecasts. Rather than comparing deterministic and ensemble forecasts, this study focuses on comparing different types of ensemble forecasts. There are multiple ways of assessing and representing forecast uncertainty. Consequently, there exists many different means of building an ensemble forecasting system for future streamflow. One such possibility is to dress deterministic forecasts using the statistics of past error forecasts. Such dressing methods are popular among operational agencies because of their simplicity and intuitiveness. Another approach is the use of ensemble meteorological forecasts for precipitation and temperature, which are then provided as inputs to one or many hydrological model(s). In this study, three concurrent ensemble streamflow forecasting systems are compared: simple statistically dressed deterministic forecasts, forecasts based on meteorological ensembles and a variant of the latter that also includes an estimation of state variable uncertainty. This comparison takes place for the Montmorency River, a small flood-prone watershed in south central Quebec, Canada. The assessment of forecasts is performed for

lead times of one to five days, both in terms of forecasts' quality (relative to the corresponding record of observations) and in terms of economic value, using the new proposed framework based on the CARA utility function. It is found that the economic value of a forecast for a risk-averse decision maker is closely linked to the forecast reliability in predicting the upper tail of the stream-flow distribution. Hence, post-processing forecasts to avoid over-forecasting could help improving both the quality and the value of forecasts.

4.2 Introduction

More than fifteen years after its advocation by Krzysztofowicz (2001) and more than a decade after the creation of the Hydrologic Ensemble Prediction EXperiment (HEPEX) community (Franz and Ajami, 2005; Schaake et al., 2007), *the case for probabilistic forecasting in hydrology* has been accepted by many researchers and practitioners across the world: uncertainty assessment of hydrological forecasts conveys important information for decision makers and therefore should be quantified and be considered as part of the forecast.

Beven (2016) distinguishes aleatory uncertainty, that originates from data only and possess stationary statistical characteristics, from various types of epistemic uncertainties. Epistemic uncertainties can arise from a lack of knowledge regarding the system's dynamics, from a lack of knowledge regarding the relevant forcings for the modeling process and also from disinformation in the data. More broadly speaking, as discussed in Juston et al. (2013), uncertainty in hydrological forecasting mainly originates from data and models (atmospheric and hydrologic). The most important sources of uncertainty in short-term hydrological forecasting are structural uncertainty (choice of a particular hydrological model structure), state variable uncertainty and parameter uncertainty, which are both linked to the availability and quality of hydro-meteorological data, and meteorological forecasts uncertainty. The latter gain in importance gradually as the forecasting horizon increases.

However, as there exists multiple sources of uncertainty in hydrological processes, there also exists many means of assessing this uncertainty and building an ensemble to represent this uncertainty. It is possible, for instance, to produce streamflow ensemble forecasts from meteorological ensemble forecasts used as inputs to at least one previously calibrated hydrological model. Deterministic forecasts can also be "dressed" using past error statistics.

While there is a general agreement among the global scientific community that ensemble and probabilistic forecasts are superior to deterministic ones (e.g. Jaun et al., 2008; Velazquez et al., 2010; He et al., 2013, and many others), there remains no consensus regarding the best means of obtaining an ensemble of streamflow forecasts (i.e. constructing the ensemble). There has also been an increased interest over the last few years in regards to assessing the economic *value* of forecasts. The quality of a forecasting system can be assessed by comparing forecasts for different lead times with corresponding observations. Forecasts quality can be further decomposed into different attributes (e.g. resolution, sharpness, discrimination...) that can be weighted differently depending on specific applications. Forecasts *value* also depend on the specific applications In particular, the usefulness of a forecast is inherently linked to the decision maker's ability to adapt their behaviour to the information provided. Neither the assessment of forecasts *quality* and *value* are straightforward and sometimes the relationship between the two is not obvious either.

In the case of hydropower production, forecast values can be assessed using sophisticated decision-making models based on stochastic dynamic programming in an operational research framework (e.g. Boucher et al., 2012; Carpentier et al., 2013; Côte and Leconte, 2016). Early flood warning is another very important application for streamflow forecasts and a decision problem entirely different from the optimization of hydropower production. Hydrologists most often, if not always, assess the value of streamflow forecasts for early flood warning using the cost-loss framework (e.g. Murphy, 1977; Richardson, 2000; Roulin, 2007; Verkade and Werner, 2011), which does not account for the decision maker's *risk aversion*, i.e. the fact that, given the opportunity, a decision maker would be willing to spend money (or resources) to reduce the amount of

uncertainty they face. This is discussed formally in section 4.3 below.

This study considers the evaluation of the economic value of early warning flood systems, from the point of view of the decision maker, with explicit consideration of risk aversion. This alternative framework is based on the use of the von Neumann and Morgenstern (vNM) utility function (von Neumann and Morgenstern, 1944), which is widely used in economics but rarely in hydrology.[1] To the best of our knowledge, our study represents the first attempt at accounting for risk aversion in the assessment of the economic value of streamflow forecasts for early flood warning. This new framework is used to assess the economic value of three concurrent streamflow ensemble forecasting systems in a case study for the Montmorency River, a flood-prone watershed in south central Quebec, Canada. Five day statistically dressed deterministic forecasts for this watershed have been issued operationally since 2008 by the Direction de l'Expertise Hydrique (DEH), a Quebec provincial agency. These forecasts are used for early flood warning and emergency response by the civil security bureau of Quebec City.

In section 4.3, some concerns regarding the cost-loss ratio are raised and an alternative framework is presented. Section 4.4 describes the context of the case study, namely the specifics of the Montmorency River watershed, the current flood forecasting system based on dressed deterministic forecasts as well as the early flood warning mechanism in place. Two variants of a concurrent flood forecasting system are detailed in section 4.4.3. The economic model is presented in section 4.5. Performance assessment metrics, both in terms of forecasts quality compared to observations, and in terms of economic value, are presented in section 4.6. Results are presented in section 4.7 and discussed in 4.8. Conclusions are drawn in section 4.9 along with suggestions for future improvement of the proposed economic model.

---

[1]Exceptions include Krzysztofowicz (1986) for seasonal water supply planning and Merz et al. (2009) for flood events, although Merz et al. (2009) use risk indicators and not vNM utility functions.

4.3 The economic model and the limits of the cost-loss ratio

The cost-loss ratio decision model (Murphy, 1977; Katz and Murphy, 1997; Richardson, 2000) is a simplified framework used in numerous hydro-meteorological studies to assess the economic value of forecasts (Roulin, 2007; Abaza et al., 2014; Verkade and Werner, 2011, among many others). As pointed out by Zhu et al. (2002), this approach is only the simplest one out of a much larger range of options. More importantly, a classical cost-loss ratio decision model disregards the role of risk aversion (e.g. Shorr, 1966; Cerdá Tena and Quiroga Gómez, 2008). "Risk aversion" refers to an attribute of a decision maker who would be willing to pay a certain amount of money to remove any risk associated to a decision problem. The specific amount of money he or she is willing to pay for this is initially unknown and can be seen as an indirect measure of the magnitude of this aversion.

As discussed by Cerdá Tena and Quiroga Gómez (2008), risk-aversion is very common, and most decision makers are risk-averse when the stakes are high. In their paper, they illustrate how disregarding risk aversion can sometimes lead to misleading conclusions regarding the value of information (such as meteorological or hydrological forecasts). Their framework also involves the Constant Absolute Risk Aversion utility function (see section 4.3). However, the context of their application and the rest of their economic model is different from ours.

In a simple cost-loss ratio, the decision model follows a contingency table that allows for binary decisions, with known associated costs. When applied to ensemble forecasts, decision-making according to the cost-loss ratio framework is based solely on a probability threshold associated to the material consequences of the event of interest (e.g. a flood event), regardless of the ensemble spread (uncertainty). Appendix A illustrates a technical presentation that builds on the concepts presented in this section. Including the concept of risk aversion in the decision model is not only more realistic, but allows weighting the ensemble members differently depending on the level of

risk aversion. For instance, a risk-averse decision maker will give more importance to the forecasts members in the upper tail of the predictive distribution (i.e. highest streamflow values).

In economics, "utility" is an ordinal notion that reflects the decision maker's preferences over a set of possible outcomes. Preferred outcomes lead to greater utility values. In the context of random outcomes, the most popular class of utility functions is the von Neumann and Morgenstern (vNM) utility function, as introduced in von Neumann and Morgenstern (1944).

Fishburn (1989) provides a retrospective on von Neumann and Morgenstern theory. He enlightens the remarkable impact this theory had on the subsequent development of economic theories and also clarifies some of its limits. There exists a immense amount of literature regarding the application of vNM utility theory in many different fields. For instance, Pope and Just (1991) compare different types of utility functions to represent preferences of farmers for potato acreage. Although we could not find previous work in hydrology where risk-aversion is considered in the assessment of the economic value of forecasts, Krzysztofowicz (1986) and Merz et al. (2009) acknowledge its importance. Shorr (1966) attempts a reconciliation of the cost-loss ratio framework with utility theory in the simple context of crop protection.

The interested reader is referred to Chapter 6 in Mas-Colell et al. (1995) for more details as well as the axiomatic foundations of vNM utility functions.[2]

The vNM utility function of a decision maker regarding a real-valued random outcome $\tilde{c}$ (e.g. money) is given by:

$$U(\tilde{c}) = \sum_{m=1}^{M} p_m \mu(c_m) \tag{4.1}$$

where $m = 1, ..., M$ are the different "states of the world", p_m is the probability of state m, and c_m is the realization of the random outcome $\tilde{c}$ in state m. The function $\mu(\cdot)$ is assumed to be non-decreasing.

The set of states of the world represent the set of realizations of $\tilde{c}$ for which the decision maker

---

[2]See also Werner (2008) and chapters 1 and 2 of Gollier (2004). For an online reference, Levin (2006) proposes an excellent review of the main concepts. Available online at http://web.stanford.edu/~jdlevin/Econ\%20202/Uncertainty.pdf. (Accessed on 11/22/2016).

has preferences For instance, in Cerdá Tena and Quiroga Gómez (2008), there are only two possible states of the world: "adverse weather" and "non adverse weather". [3] In the case of flood forecasting systems, even if the streamflow values are continuous, the decision maker may only distinguish between a finite set of implied damages. This point is discussed further in section 4.5.2 where a finite number of "damage categories" are specified.

The curvature of the function $\mu(\cdot)$ reflects the decision maker's preference regarding uncertainty. If $\mu(\cdot)$ is concave, the decision maker is risk-averse; if it is linear, the decision maker is risk-neutral; if it is convex, the decision maker is risk-seeking. To see why, consider the random variable $\tilde{c}$, and its expected value $\bar{c}$.[4] Since $\bar{c}$ is not risky, a risk-averse decision maker should prefer receiving $\bar{c}$ with certainty than receiving a random draw from $\tilde{c}$. That is: $U(\bar{c}) > U(\tilde{c})$, or $\mu(\bar{c}) > \sum_{m=1}^{M} p_m \mu(c_m)$, which is the definition of concavity. Note that we can also define $C > 0$, the amount of money that the decision maker would be willing to spend to remove the risk associated with $\tilde{c}$, as follows:

$$\mu(\bar{c} - C) = \sum_{m=1}^{M} p_m \mu(c_m) \tag{4.2}$$

This argument extends directly to any change in risk: any risk-averse decision maker prefers less risky distributions, in the sense of mean-preserving second order stochastic dominance (Rothschild and Stiglitz, 1970). Figure 4.1 also presents a graphical version of the above discussion when there are only two states of nature.

---

[3] vNM utility functions can also account for an infinite number of states of the world. In such case, one would have: $U(\tilde{c}) = \int \mu(c)f(c)dc$, where f is the pdf of $\tilde{c}$.

[4] Note that $\bar{c}$ can be thought as a degenerated random variable, taking the value $\bar{c}$ with probability 1.
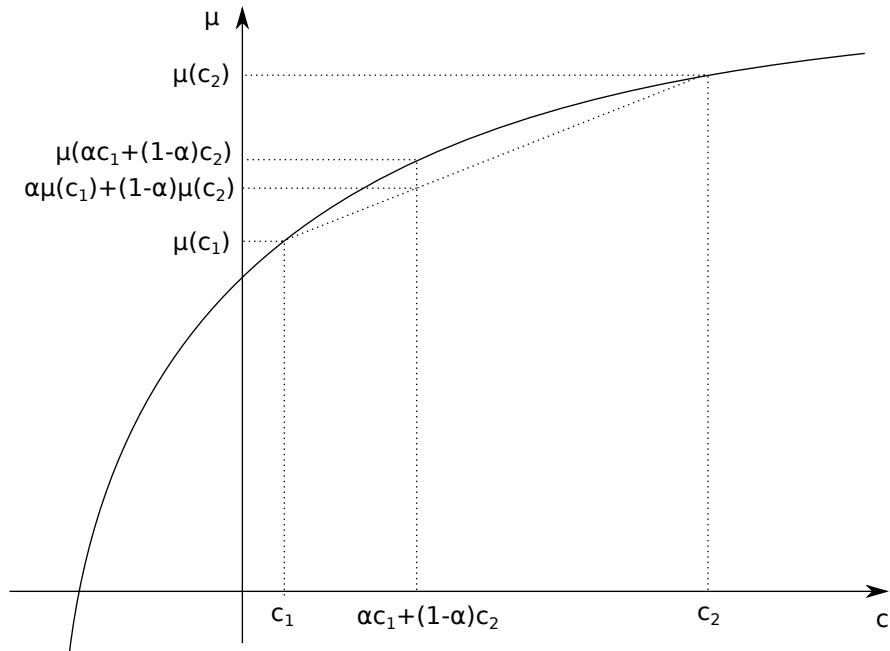
Figure 4.1: A schematic representation of the CARA utility function for risk-averse individuals. Here, only two states of the world are assumed. The state c_1 is realized with probability α and c_2 is realized with complementary probability. Since μ is concave, we see that the expected utility $U = \alpha\mu(c_1) + (1-\alpha)\mu(c_2)$ is smaller than the utility of the expected value $\mu(\alpha c_1 + (1-\alpha)c_2)$. In other words, the individual would prefer receiving the certain amount $\alpha c_1 + (1-\alpha)c_2$ than receiving a lottery which pays c_1 with probability α and c_2 with probability $1-\alpha$. Equivalently, the individual would be willing to pay *up to* $C = \mu(\alpha c_1 + (1-\alpha)c_2) - [\alpha\mu(c_1) + (1-\alpha)\mu(c_2)] > 0$ to remove the risk associated with this lottery.

This study focuses on a well-known parametric family for $\mu(\cdot)$ known as the Constant Absolute

Risk Aversion (CARA) function, given by Eq. 4.3.

$$\mu(c) = \frac{-\exp(-Ac)}{A} \qquad (4.3)$$

where *A* is the risk aversion of the decision maker. *A* is strictly positive for risk-averse individuals and strictly negative for risk-seeking individuals. For positive value. the level of risk aversion increases when *A* increases.

The parametric form in Eq. 4.3 implies that the level of risk aversion is independent of the decision maker's financial capacities (hence the name *Constant Absolute* Risk Aversion, CARA). This particular utility function is therefore coherent with the expected behaviour of most public utility services (municipal authorities will not, for instance, gradually adopt a risk-seeking behaviour regarding the protection of citizens if the city's financial well-being improves). See Appendix B for additional details, proofs, and references for those claims.

The economic model developed above is applied to the particular context of frequent flooding on the Montmorency watershed. This context is described in greater details in the next section.

4.4   Context

4.4.1   Floods on the Montmorency Watershed

Located in southern Québec, Canada, the Montmorency River watershed covers 1150 km^2, most part of which is densely forested. Approximately 30 000 people reside in the basin, concentrated in its southernmost portion. The northern portion of the watershed lays within the Laurentian Wildlife Reserve, where heavy snowfall precipitation is common. Figure 4.2 presents the average monthly values for meteorological variables for this watershed.
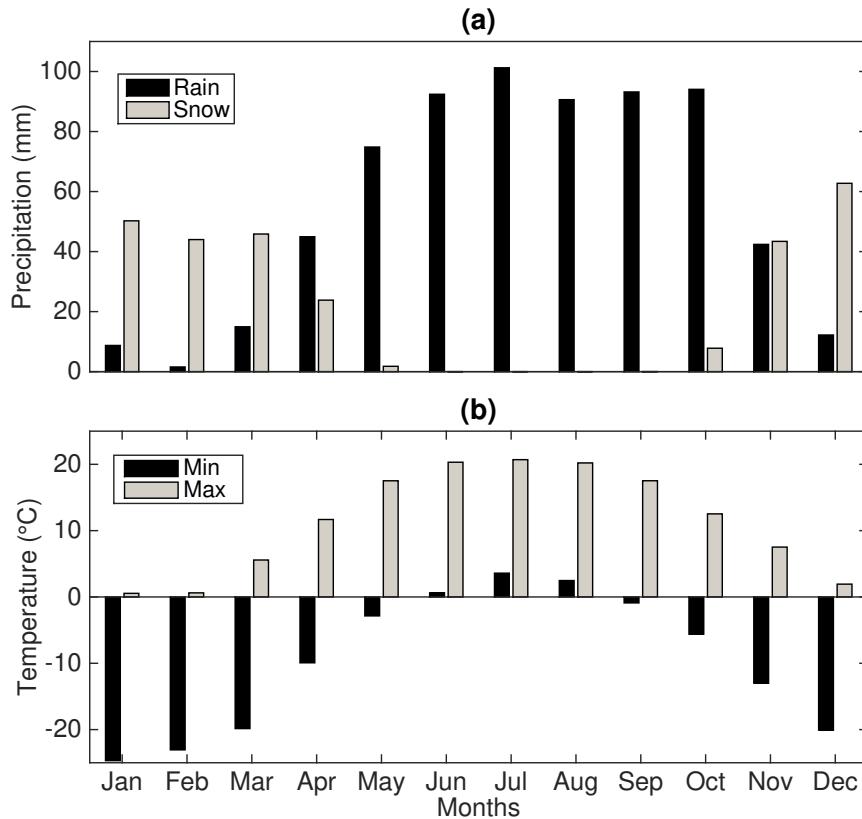
Figure 4.2: Monthly average values for (a) precipitations and (b) temperature for the Montmorency River watershed

Crystalline rock of the Canadian Shield covers most of the watershed, where the retreat of glaciers left till of an average thickness of 1 m. The southernmost part is covered in sandy sediments from the Champlain Sea. Figure 4.3 shows the geographical location of the watershed as well as the location of the available meteorological stations and streamflow gauges (see section 4.4.3).
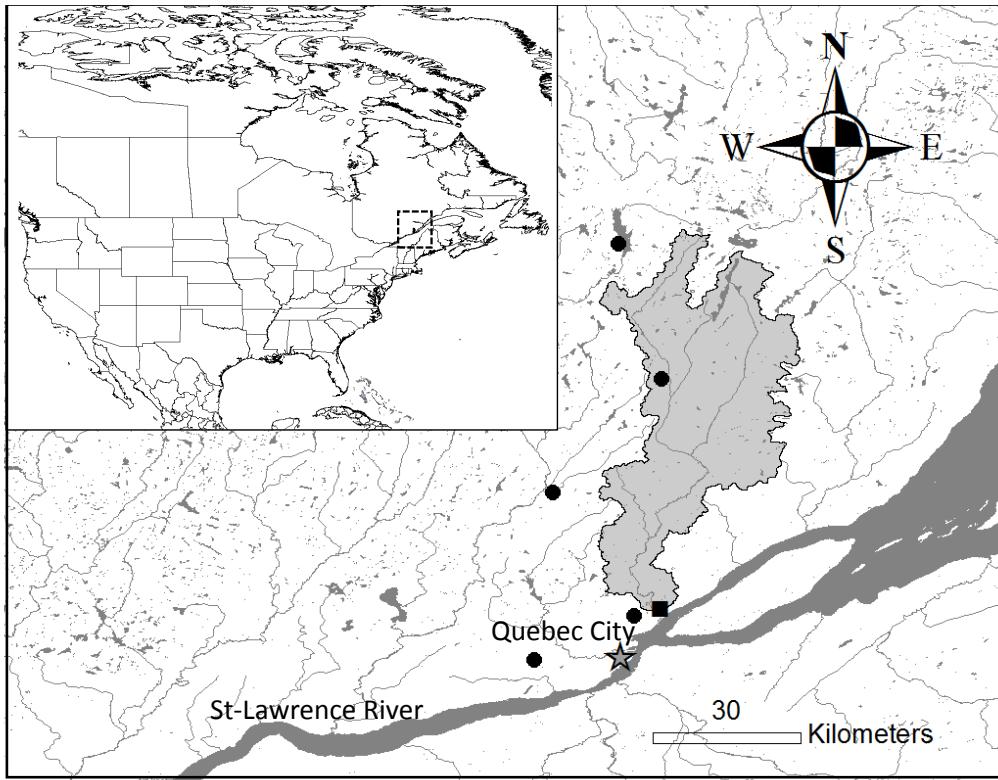
Figure 4.3: Geographical location of the Montmorency watershed. The black dots represent the available meteorological stations and the black square is the streamflow gauging station.

The Montmorency River experiences quasi-annual ice jams during spring melt, which often enhance the magnitude and frequency of floods within vulnerable inhabited areas. The response time of the watershed is rapid (12 hours). The return period of damaging floods is also short. This makes emergency evacuation and flood damage a common occurrence for riverside residents. Table 4.1 shows return periods and corresponding streamflow values for the Montmorency River (Leclerc and Secretan, 2012). The table also provides thresholds for streamflow values used for flood mitigation operations (see section 4.4.2.2). Note that these are given for open-water levels, and take neither ice jams nor the increase in water level due to the presence of ice blocks into account.

The behaviour and consequences of ice jams along the Montmorency River have been the focus

Table 4.1: Streamflow associated with important return periods and flood mitigation thresholds for the Montmorency River watershed.

Return period (years)	Threshold (m^3/s)	Streamflow
	Surveillance: Close surveillance of river behaviour	350
2		439.0
	Pre-Alert: Warning calls to emergency employees	450
	Alert: Mobilization	500
	Flood: Active evacuation	550
5		569.3
10		655.6
25		764.7
50		845.6
100		925.7
1000		1191.2
10 000		1456.0

of previous studies, such as forecasting river ice breakup (Turcotte and Morse, 2015). Risk analysis and technical solutions (Leclerc et al., 2001) have also been studied, but as of yet not implemented.

The river experienced its worst recorded event in 1964, when a heavy rain system melted a late autumn snow cover, resulting in a 1100 m^3/s flow peak. More recently, an ice cover breakup followed by the formation of an ice jam formation further downstream in January 2008 forced the evacuation of 80 households and damaged four houses. In March 2012, an early spring thaw caused by extreme temperatures induced a flood resulting in the evacuation of 25 households. Then, in April 2014, an ice jam breakup caused a massive ice-carrying flood wave that, occurring during a typical normal spring freshet, quickly raised waters to a semi-centennial level. In addition, the topography in the area causes certain regions to become entirely isolated and surrounded by water during flooding. The greatest concern of public authorities occurs when people refuse to evacuate, especially in these flood-prone areas.

4.4.2   Current forecasting and decision-making process

4.4.2.1   The hydrological model HYDROTEL

HYDROTEL (Fortin et al., 1995) is a spatially distributed, physics-based model developed and maintained by the Institut National de Recherche Scientifique (INRS). It is used operationally by the DEH, and has been implemented in the Montmorency River watershed since 2008 (Rousseau et al., 2008). The model accepts gridded inputs (precipitation, snow cover, temperature) than can be interpolated using a three station average or Thiessen method. Physical features of the catchment (topography, soil type, hydrographic network) are processed by a companion software called PHYSITEL. It divides the watershed in smaller spatial units called RHHU (Relatively Homogeneous Hydrological Units). Each of the RHHU is then assumed to possess homogeneous physical properties. HYDROTEL then performs the computation of vertical and horizontal water flows.

HYDROTEL offers a range of sub-routines for hydrological processes (interpolation of precipitation, evapotranspiration, snow accumulation and melt, etc.). The user chooses the most appropriate sub-routines depending on the available data. For this study, interpolation of observed precipitation was performed using Thiessen's polygons. No radiation data were available, so evapotranspiration was estimated from an empirical temperature-base method (Fortin, 2000; Bisson and Roberge, 1983) and snowmelt was modelled by a mixed degree-day/energy budget approach. The vertical water budget was performed by the sub-routine BV3C (in French *Bilan Vertical en 3 Couches*) that divides the soil into three layers of different composition and depths. Both overland and channel routing was performed using the kinematic wave approach (Lighthill and Whitham, 1955). With this setup, which replicates the model setup used operationally by the DEH, HY-DROTEL has 27 parameters, but only 10 were calibrated (default values were used for the other parameters). The calibration already performed by the DEH was kept intact. This calibration was performed using the Shuffle Complex Evolution algorithm of the University of Arizona (SCE-UA,

Duan et al., 1994). The objective function to maximize was the Nash-Sutcliffe Efficiency criterion. In forecasting mode, HYDROTEL is driven by meteorological forecasts, either deterministic or ensemble-based.

In the actual operational setting, data assimilation is performed manually and indirectly: the forecaster modifies precipitation and/or temperature observed during the previous days until the model's simulation is in agreement with the observed streamflow for the actual day. When the model is run with the modified meteorological inputs, state variables are re-computed and should translate into an improvement of the model's description of the hydrological state of the watershed. The choice of applying modifications to temperature or to precipitation depends mostly on the period of the year and associated dominant hydrological that is processed. Thus, during spring freshet, air temperature is the main forcing that acts on the snow melt rate. Solar radiation is not among HYDROTEL's inputs but is rather estimated empirically, in part through air temperature. Therefore, during this period of year (early March to late May), perturbations are applied on temperature forcing. During the summer and early fall periods, precipitation forcing is the dominant factor for controlling runoff, soil moisture and eventually streamflow. Perturbations are applied primarily on precipitation from approximately June to November.

4.4.2.2 Flood alerts

The Direction de l'Expertise Hydrique (DEH) is an administrative unit of the Government of Québec created in 2001 with the mandate to manage the water regime of Québec's rivers and provide streamflow forecasts to municipalities. Since 2008, operational five day, three hour time step streamflow forecasts are distributed to municipal water managers. Those forecasts are always obtained using the semi-distributed physics-based hydrologic model HYDROTEL (Fortin et al., 1995). Although HYDROTEL is a deterministic model, the operational forecasts now largely distributed by the DEH are not purely deterministic but are rather accompanied by a 50% confidence

interval. This confidence interval is computed from a statistical model derived from the analysis of past deterministic streamflow forecasts errors for 10 watersheds across the province of Québec. A more detailed description of this statistical method is available in Huard (2013).

After receiving a forecast exceeding a pre-determined flood threshold, municipalities can choose to engage in emergency procedures. In the case of the Montmorency watershed, current measures are mostly reactive (road closure, controlled evacuation of citizens, providing emergency shelters and food) rather than preventive (artificial levees, culverts, etc., Leclerc et al., 2001).

Flood thresholds have been adapted from an hydrodynamic study (Leclerc and Secretan, 2012). Threshold numbers have been conservatively rounded down to compensate for the worsening effect of ice in the channel. Table 4.1 includes operational threshold levels for the most vulnerable residential area.

4.4.3   A concurrent flood forecasting framework based on meteorological ensemble forecasts

4.4.3.1   Meteorological ensemble forecasts

The alternative forecasting framework proposed in this study involves meteorological ensemble forecasts passed on to HYDROTEL. Precipitation and temperature ensemble forecasts from the Meteorological Service of Canada (MSC) covering the 2011—2014 period are used. For practical reasons, those forecasts were obtained from the THORPEX[5] Interactive Great Grand Ensemble (TIGGE) database managed by the European Center for Medium Range Weather Forecasts (ECMWF). The forecasting horizon is five days, with a six hour time step. The MSC meteorological ensemble forecasts comprise 20 members. The initial spatial grid of $0.6°$ was downscaled to a

---

[5]THe Observing system Research and Predictability EXperiment. It is a program led by the World Meteorological Organization.

0.1° grid through simple bi-linear interpolation during data retrieval.

Observations for precipitation and temperature are measured at five ground stations distributed around the watershed (see Figure 4.3). Hourly measured data was accumulated and averaged over a three hour time step. Snow survey data interpolated on a 0.1° grid are also available. They were provided for this study by the DEH. The streamflow gauging station at the river outlet provides measurements at a 15 minute interval, corrected for backwater due to ice cover and then averaged over three hour time steps.

4.4.3.2   Data assimilation and state variable uncertainty

Appropriate data assimilation is crucial for short-term flood forecasting as it allows the model to begin the forecasting period having the best possible estimate for initial conditions. In a study involving 20 catchments in Quebec, Thiboult et al. (2016) showed that the uncertainty for initial conditions dominates the other sources of uncertainty for short-term (1-day to 3-day ahead) streamflow forecasts.

In this study, manual data assimilation was performed according to the guidelines by Mamono (2010) and agree with the procedure followed by operational forecasters at the DEH. This assimilation process relies on the assumptions that: (1) model errors are entirely compensated by the model calibration process, (2) streamflow measurements are error-free, and (3) the only remaining source of error affecting state variables is attributable to meteorological inputs (Mamono, 2010). Additive coefficients were applied to temperature inputs while multiplicative coefficients were applied to precipitation inputs in order to improve the agreement between simulated and observed streamflow series. Those perturbations were respectively bounded at [-10,10] and [0.1, 10]. Although those minimal and maximal perturbation values are very large, they truly correspond to the rules applied by the DEH operationally. Of course, the goal is to limit perturbations as much as possible. In this study, the multiplicative coefficient applied to precipitation varied between 0.5 and 2.5. Most

additive coefficients for temperature varied between -3 and +2.5, with occasional larger coefficients (up to -7 and +7, on three occasions). Those perturbations of meteorological inputs were applied uniformly onto the basin for fixed periods of time.

The manual data assimilation described above only improves on the "best guess" of the state variables for each time step. To go one step further, additional perturbations were applied around this best guess estimate in order to account for the uncertainty of initial conditions. To do so, a rudimentary Ensemble Kalman Filter (EnKF, Evensen, 2003) was implemented. From the starting point—constituted by manually assimilated precipitation, temperature and streamflow simulation series—random noise is further applied to precipitation and temperature inputs. Additive perturbations are drawn randomly from $U(-8,8)°$ for temperature. For precipitation, both multiplicative ($U(0.5,1.5)$) and additive ($U(0,0.5)$ mm) perturbations are drawn. The inclusion of additive perturbations for precipitation is due to the fact that strong under-captation is suspected for this catchment. Output uncertainty is modelled by a normal distribution centered on observed streamflow with a standard deviation taken as 10% of the observed streamflow. In this study, data assimilation is a necessity rather than a choice and is not at all the primary objective. For this reason, the limits of the above-mentioned distributions were not optimized as in Thiboult and Anctil (2015). Those limits were fixed according to the guidelines in Mamono (2010) and Abaza et al. (2015) and the experience gained during manual data assimilation. Further refinements of the EnKF model is outside the scope of this study.

The Kalman gain K is computed following Mandel (2006)

$$K_t = M_t H^T (H M_t H_t^T + O_t)^{-1} \tag{4.4}$$

where M_t is the model error covariance matrix computed according to the perturbations defined above and O_t is the covariance of observation noise also computed according to the perturbations drawn from the normal distribution described above. The matrix H relates the state vectors and observations (so called "observation model"). It can be demonstrated through matrix algebra that

Eq. 4.4 amounts to computing the derivative of the analysis error and setting it equal to zero.

Once the Kalman gain is computed, it is used to weight the credibility of the model error $z_t - HX^-$ relative to the a priori estimation of state variables X^- according to Eq. 4.5. This leads to the updated model states, X^+.

$$X_t^+ = X_t^- + K_t(z_t - HX_t^-) \tag{4.5}$$

The next section adapts the general framework presented in section 4.3 to the specifics of the Montmorency watershed.

4.5 Parametrization of the economic model

The preferences of a decision maker with risk-averse preferences represented by a CARA utility function can be represented as follows:

$$U(s) = \sum_m p_m \frac{-1}{A} \exp\left\{ -A\left[-d(Q_m) + b\big(d(Q_m), s, w\big) - s \right] \right\} \tag{4.6}$$

Strictly speaking, each ensemble member Q_m has a probability of occurrence p_m, and corresponds to a given damage $d(Q_m)$. In this study, the damage curve is broken down into 12 categories (i.e. $m = 1, ..., 12$). This choice of 12 categories it is based on a previous hydraulic study by Leclerc and Secretan (2012) to establish inundation maps. They produced 11 maps, for streamflow varying from 550 to 1050 m^3/s with an increment of 50 m^3/s. This increment of 50 m^3/s, is adopted here, but all thresholds were reduced to be in agreement with streamflow values that induced inundations (see also the operational thresholds mentioned in Table 4.1). The first category represents all the "no flood" category (i.e. below the lowest threshold).

Then, Q_m represents the streamflow associated with the mth category and p_m becomes the probability associated to this category, inferred from the number of members that fall within it. Given s,

the amount of money spent (w days ahead, see section 4.5.3 below) on flood emergency measures, the resulting gain (or benefit) in terms of damage reduction is given by $b\big(d(Q_m), s, w\big)$.

While Q_m and p_m are derived directly from the ensemble forecast, d, s and $b\big(d(Q_m), s, w\big)$ must be calibrated from other sources of information related to actual operation and decision history. This can be a challenge, but fortunately in the case of the Montmorency River, a record of citizen evacuations and corresponding spending for the 2014 flood was available. Although incomplete, this record allows us to guide the estimation of d, s and $b\big(d(Q_m), s, w\big)$.

In this context, the cost of the implementing and operating the forecasting system as such is not considered in s. Of course, when the civil security chooses which forecasting system to put in place, they must consider the cost of implementing this particular system. Nevertheless, once the system is in place, its cost should not affect precautionary spending decisions. This also motivated the choice of CARA utility functions, since they do not depend on "wealth" (which would be affected by the cost of performing the forecast).

4.5.1   Level of risk aversion A

Risk aversion A is an intrinsic characteristic of each person or organization and could be calculated, given the availability of a sufficiently long record of decisions and associated money spending. However, in the present study, A was left free for the following reasons. First, the available data is not sufficient to credibly calibrate A. Second, as one of the goals of this study is to illustrate how risk aversion influences the value of a forecasting system for a particular problem, it is logical to cover a range of possible As, including the risk-neutral $A = 0$ situation. Therefore, A was made to vary from 0 to 0.01. Although these represent relatively small levels of risk aversion (Babcock et al. (1993)), preliminary tests have shown that, in the context of this paper, these values were sufficient to illustrate a change in the decision maker's spending decisions and therefore on the economic value of the concurrent forecasting frameworks. Negative values for A were not considered, as they

represent a risk-seeking decision maker, unrealistic in the context of flood mitigation.

4.5.2 Damages d, spending s and damage reduction b

The material damages to houses and property associated with flood events can be estimated using the flow-damage curve established by Leclerc et al. (2001). This curve is based on a survey regarding the types of houses in the sector: one or two stories, with or without basement, etc. and their value according to the municipal evaluation. The level of submersion for different streamflow values were obtained through hydraulic simulations. The damage is then deduced from this level of submersion using Gompertz' law (Gompertz, 1825). The damage expressed in dollars rises exponentially with observed streamflow (m^3/s) and range from \$0 to \$375 000.

In this study, the following parametrization of the benefit function is used:

$$b\big(d(Q_m), s, w\big) = \min\big\{\beta_w \cdot s, \psi \cdot \hat{d}(m)\big\} \tag{4.7}$$

where $d(m) = \psi\hat{d}(m)$, $\hat{d}(m)$ is the flow-damage curve (Leclerc et al., 2001) for the forecast member m, and β_w and ψ are parameters. This particular parametrization assumes that the benefit of spending is linear, until all damages are avoided. It also implies that it is never optimal to spend more than $\max_m\{\psi \cdot \hat{d}(m)\}$, since additional spending brings no additional benefit, for any possible forecast member.

The parameter β_w has been initially calibrated by assuming $\psi = 1$. By comparing the total amount of money spent in 2014 to alleviate flood damages with the damages (in dollars) predicted by the aforementioned damage curve using the observed streamflow, it was found that the calibrated β_w was less than one. This implies that the civil security service would have spend more than the total amount of possible damage.

This therefore implies the existence of intangible benefits associated with having a flood warn-

ing system and spending money to mitigate flood effects. According to Lave and Lave (1991) and Carsell et al. (2004), these intangible benefits include but are not limited to: not putting people's health and security at risk, stress reduction for the population, and building a feeling of trust towards the authorities. In the case of the Montmorency River, there has never been any loss of life. However, as mentioned earlier, it may happen that people refuse to leave their residences and become isolated from communicating roads restricting their access to services and medical care. Unfortunately, it is very difficult and probably rather imprudent to associate a definite cost to these intangible benefits such as "reducing stress". In the absence of a better alternative, in this study a multiplying factor ψ was applied to the damage curve to account for those intangible benefits, as suggested in Van Dantzig and Kriens (1960). The parameter ψ was made to vary between 1.5 to 10 and β_w was computed again for each different value of ψ, as the damage curve is modified. The lower limit of ψ was set so that money spent during the flood of 2014 equals the damage predicted by the damage curve. Therefore, in this framework, the damage curve of Leclerc et al. (2001) (i.e. $\hat{d}(m)$) represents mostly the relationship between streamflow and its impact on the lives and well-being of people.

4.5.3   Warning time and dynamic decision-making

According to the US Army Corps of Engineers (1994), as well as to Richardson (2000) and Roulin (2007), the costs of emergency measures or benefits thereof are related to warning time w. In particular, Roulin (2007) assumes that early action can reduce the total cost of emergency measures and maximize damage reduction. Carsell et al. (2004) also provide an evaluation of residential content (furniture, food, electric appliances, etc.) that can be protected with a given warning time.

However, the accuracy of forecasts is inversely related to lead time and the decision maker might want to wait for better information before taking a decision.

Those considerations go far beyond the objective of this study, and the formalization of an

explicit dynamic decision process is left for further research. In this study, the dynamic nature of the problem is addressed by assuming that the decision maker uses the following myopic decision procedure:

1. At the beginning of each day, the decision maker receives a 5-day forecast.

2. Iteratively, and starting with the *earliest* (5-day) forecast, the decision maker chooses their preferred level of spending. This level of spending is chosen as to maximize Eq. 4.6.

3. The decision maker is constrained (by external factors such as the availability of materials or labour force) to spend at most a fraction δ of their preferred level of spending s (see below).

The benefits of a spending are assumed to take effect on the day the spending decision is made, up until the forecast date. For example, if a decision maker spends \$1000 on a given Monday, anticipating a flood the following Thursday (i.e. a 4-day forecast), then any damage occurring prior to Thursday is also reduced (by $\beta_w \times$ \$1000).

The parameter β_w is divided between lead times according to $[2, 1.75, 1.5, 1.25, 1]\beta_{2014}$, where β_{2014} is calibrated on the spending decisions of 2014 and represents the baseline ratio of gain per dollar invested. The above multiplication therefore assumes that early actions lead to higher gains per dollar spent. This is very similar to the methodology presented in section 4.3 of Roulin (2007), except that only one repartition of β_w is tested here compared to two in Roulin (2007).

If the decision maker is to take successive actions at different lead times according to forecasted streamflow, then the total amount of available money can be spread across lead times. The decision maker can, for instance, spend all the available money two days prior to the event. Or, they can spend half two days prior and the remaining half the day before the flood (1-day). To account for this, five different "spending vectors" were created (Table 4.2). The values in those spending vectors represent the maximal fraction δ of the preferred level of spending s that can be spent at each lead time. The first three spending vectors represent situations for which there is no limit on the spending than can be made the day before, with spending vector number 3 representing

the extreme case where the decision maker *must* wait until the 1-day forecast before spending any money. On the contrary, spending vectors number 4 and 5 represent a fictitious situation in which the decision maker can spend any amount of money at the 5-day horizon, and no spending is allowed the day before (1-day).

Table 4.2: Maximum fraction of total spending s allowed depending of the forecasting horizon. Each spending vector is identified by an identification number (ID) for further reference.

ID Number	Maximum fraction of spending allowed				
	Day 5	Day 4	Day 3	Day 2	Day 1
"No limit for a 1-day forecast"					
1	1	1	1	1	1
2	0	0.25	0.5	0.75	1
3	0	0	0	0	1
"No limit for a 5-day forecast"					
4	1	0.75	0.5	0.25	0
5	1	0	0	0	0

It is important to note that due to the myopic decision-making procedure, the decision maker does not take into account the fact that money spreads across lead times when making a decision. This effect alone underestimates the value of early spending. However, the decision maker also does not consider the reduction in uncertainty gained by waiting (which overestimates the value of early spending). In this study, those two effects are assumed to balance each other.

To summarize, the simulation procedure is as follows:

1. Fix A and ψ

2. Given the spending decision of 2014, infer the value of β_{2014} (given the decision model).

3. Given A, ψ, β_{2014} and the other model parameters, apply the decision-making procedure described in section 4.5.3 for each forecast.

4. Compute the measures of performance assessment (see section 4.6).

4.6 Performance assessment

4.6.1 Forecast quality

The three forecasting systems described in sections 4.4.2 and 4.4.3 are compared to each other by assessing their respective abilities to forecast observed streamflow values for the 1- to 5-day projections. This performance assessment also involves the well-known Continuous Ranked Probability Score (CRPS, Matheson and Winkler, 1976) and a reliability diagram (Stanski et al., 1989).

4.6.2 Evaluating the benefits of forecasts

As described in the introduction, the usefulness of an early flood warning system is in helping the decision maker choose the best spending level s, prior to the event. The value of such system is therefore closely related to the decision maker's ability to affect the outcome through their spending decisions. The benefits of forecasts are therefore evaluated with an explicit concern for the decision maker's preferences.

In order to develop an indicator of the economic benefits of a forecast, it is important to distinguish between the decision maker's *ex-ante* utility (before the uncertainty is resolved, as in Eq. 4.6) and their *ex-post* utility (the realized level of utility, after the uncertainty is resolved). This is important as spending decisions are based on the *ex-ante* utility, whereas the value of the forecasts are based on the (expected) *ex-post* utility, conditional to spending decisions. Given the spending decision s and the realized state m, the *ex-post* utility of the decision maker is given by:

$$U_m(s_f) = \frac{-1}{A} \exp\left\{ -A\left[-d(Q_m) + b\big(d(Q_m, s_f, w) - s_f\big)\right]\right\} \tag{4.8}$$

where s_f is the total amount of money spent, from a decision based on forecasts (f). The value of this *ex-post* utility is dependent, of course, of the realized streamflow values. In order to obtain a

sensible evaluation of the decision maker's utility, one must therefore consider the average *ex-post* utility:

$$\mathbb{E}_m U_m(s)$$

where the expectation $\mathbb{E}_m$ is taken with respect to the historical streamflow values. Note that, strictly speaking, the history under consideration should be long enough to be representative of the true distribution of streamflow. On the one hand, it is expected that a longer record will provide a better empirical estimate of the true streamflow distribution. On the other hand, there can also be various sources of non-stationarity affecting the observed streamflow values over time (e.g. changing the measurement apparatus, climate change, land-use change, etc). Hence, even with a very long historical record, the true distribution of streamflow cannot be known with certainty. (Note that this also affects measures of quality, such as the CRPS.)

The average *ex-post* utility can be computed for any of the three forecasting systems described in sections 4.4.2.2 and 4.4.3 but also for two special cases: perfect forecasts and no forecasts. On one hand, if forecasts were perfect, there would be no missed events and the decision maker would spend only the exact amount of money necessary to obtain the maximum possible protection, as early as time allowed. On the other hand, if no forecasts were available, there would be no decisions to be made and no money to be spent on flood mitigation and protection measures. Therefore, the maximum amount of damage would occur for each flood event.

It is important to note that utility is an ordinal quantity that only represents the preference of a person faced with a decision-making problem, given some information from uncertain forecasts. That is, the utility levels can be compared, but the actual value of the decision maker's utility has no interpretation. Consequently, the utility values computed for the three forecasting systems can be scaled relative to the utility of a perfect forecasting system. This simplifies the interpretation, without imposing any additional restriction.

The hit rate and the overspending index, two standard measures of the economic performance are also presented.

The hit rate, given by Eq. 4.9, is the ratio of avoided damages when decision-making is based on the forecasting system being evaluated to the damages that would be avoided if the forecasts were perfect (always equal to the observations).

$$Hit\ Rate = \frac{\mathbb{E}_m b\big(d(Q_m), s_f, w\big)}{\mathbb{E}_m b\big(d(Q_m), s_p, w\big)} \tag{4.9}$$

where s_p is the amount of money that would have been spent if perfect forecasts would have been available. s_f is the total amount of money spent when decisions are based on forecasts, as in Eq. 4.8. s_p matches exactly the damages corresponding to the observed streamflow, for all time steps.

Overspending is defined as in Eq. 4.10. It allows for measuring how much the forecasting system being evaluated overspends (in percentage) compared to perfect forecasts. One should aim for the overspending value to be as low as possible.

$$Overspending = \frac{\mathbb{E}_m s_f - \mathbb{E}_m s_p}{\mathbb{E}_m s_p} \tag{4.10}$$

Results are presented in the next section.

4.7   Results

4.7.1   Assessment hydrological forecasts relative to observations

Figure 4.4 displays hydrographs for a two-week period during the spring of 2014. Panels (a), (c) and (e) correspond to 1-day forecasts while panels (b), (d) and (f) correspond to 5-day forecasts. In all cases the time step is three hours. Forecasts along the upper row (a and b) are dressed deterministic

forecasts. Forecasts along the middle row are based on meteorological ensemble forecasts without EnKF while forecasts on the bottom row are also based on meteorological forecasts but account for state variables uncertainty through EnKF. This figure shows that for 1-day forecasts, forecasts based on meteorological ensembles generally have low spread. This is expected, as only the forcing uncertainty is accounted for and this uncertainty requires more than one day to be propagated through the hydrological model. In addition, at short lead times the members of meteorological ensemble forecasts are often very similar. However, before each of the two flood peaks, they display more dispersion than dressed forecasts. The influence of the EnKF can also be seen. The spread of the forecasts with EnKF is greater than the forecasts without EnKF and the density of forecasts members is higher around the observed streamflow. At the 5-day lead time, some members of the forecasts based on meteorological ensembles reach very high streamflow values. This is not the case for the dressed deterministic forecasts that often underestimate streamflow.
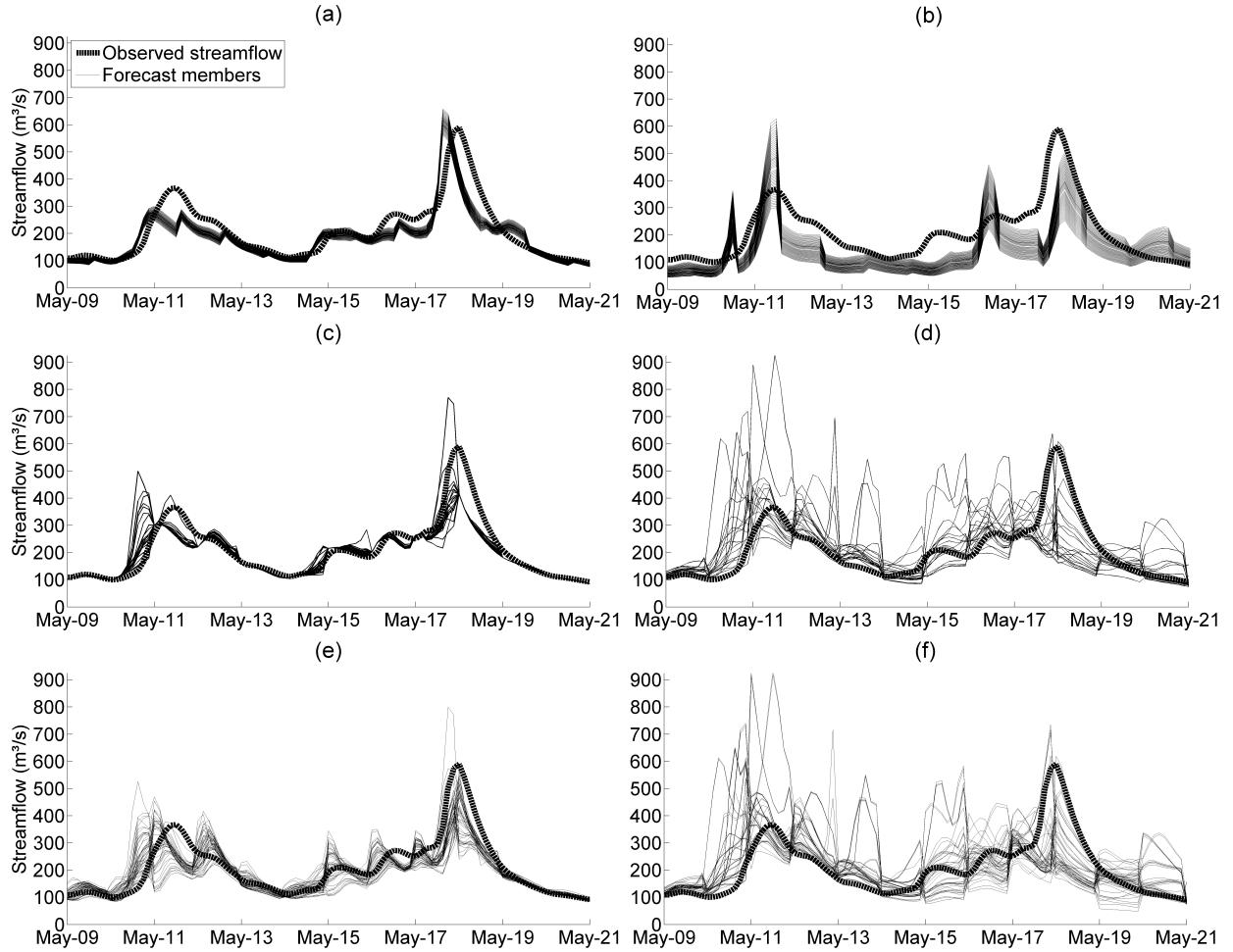
Figure 4.4: A portion of the 1-day (left) and 5-day (right) forecasted three hour time step hydrograph in 2014 against the observed streamflow; (a) and (b) are dressed forecasts, (c) and (d) are forecasts based on meteorological ensembles without EnKF and (e) and (f) are forecasts based on meteorological ensembles with state variables uncertainty estimated using the EnKF.

Figure 4.5 presents the mean CRPS of the three concurrent forecasting systems over the 2011—2014 period. The CRPS was computed separately for each lead time in three hour increments and averaged over the entire record of forecasts and corresponding observations. For very short lead times, the dressed deterministic forecasts outperform those based on meteorological ensembles (lower CRPS). As noted above, for short lead times the members of the meteorological ensemble

55

forecasts are often very similar and the forecasts thus have no dispersion. Dressed forecasts, by definition, necessarily have more spread. Since the forecasting system is not perfect, an ensemble with very low spread is at risk of missing the observation. However, for lead times longer than 18 hours, forecasts based on meteorological ensembles achieve a better (lower) CRPS than dressed forecasts, despite the jumpy behaviour of the ensemble curves compared to that of the dressed forecasts. Furthermore, the performance gap between meteorological ensemble-based forecasts and dressed forecasts increases with lead time.
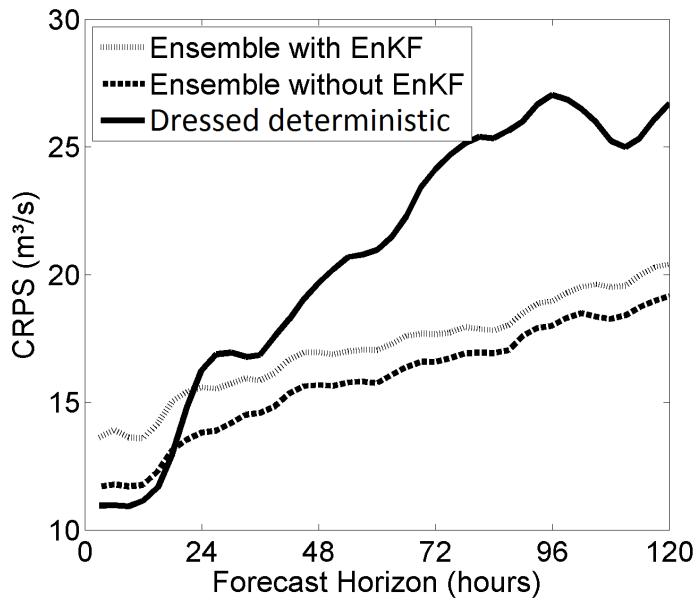

Figure 4.5: Mean CRPS as a function of lead time for the 2011-2014 period for the forecasts based on meteorological ensembles with (grey line) and without (dashed black line) state variable perturbations and for the dressed forecasts (solid black line).

The perturbation of state variables after manual data assimilation increases (worsens) the CRPS. This is likely attributable to a loss of resolution. Although sharpness, resolution and reliability are all desirable attributes of a forecasting system, there is most often a trade-off between the resolution and reliability. Sharpness is akin to "precision" and refers to the quality of a forecasting system which issue forecast members that are all close together. Resolution is is the ability of

56

the forecasting system to distinguish between different situations. Indeed, Figure 4.6 highlights that forecasts based on meteorological ensembles having a perturbation of state variables display a better reliability than when state variables remain unperturbed. The difference is most striking for 1-day forecasts. Figure 4.6 also shows that dressed deterministic forecasts are more reliable than forecasts based on meteorological ensembles for short lead times (e.g. one day, hollow circles), but less so for longer lead times (e.g. 5-day, hollow triangles). As lead time increases, the accuracy of meteorological forecasts decreases. However, the spread of forecasts based on meteorological ensembles increases considerably with lead times therefore more often including the observed values at the 5-day lead time compared to the 1-day lead time.
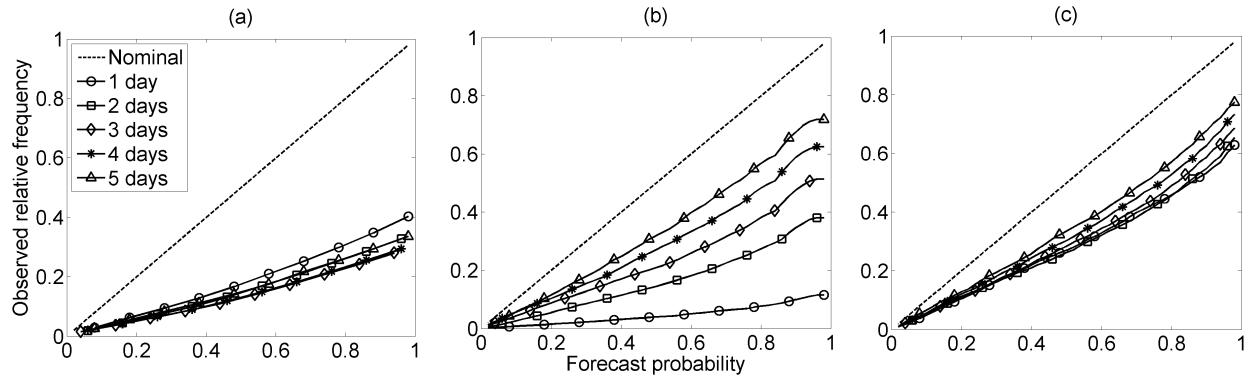
Figure 4.6: Reliability diagrams as a function of lead time for (a) dressed deterministic forecasts (b) forecasts based on meteorological ensembles and manual data assimilation and (c) forecasts based on meteorological ensembles, manual data assimilation and additional perturbation of state variables.

4.7.2 Assessment of hydrological forecasts in terms of economic value

For each of the simulated values of A and ψ, the application of each spending vector (c.f. Table 4.2) was tested over the study period (2011-2014). This section describes the simulation procedure.

An example of the applied methodology and corresponding results is provided in Figure 4.7. The upper row shows 5-day forecasts from the three systems, starting on May 17, 2014. The lower row shows how each member of each forecast is classified into 12 severity classes ranging from non-damaging (class 1) to centennial-scale flooding (class 12) defined after the damage curve.
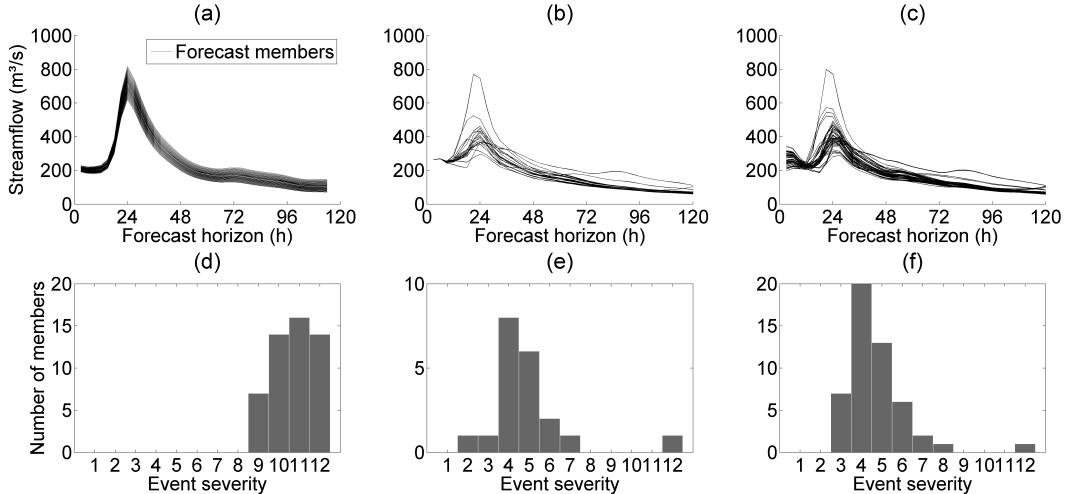
Figure 4.7: Separation of forecast members into 12 categories according to the magnitude of streamflow. The example is for forecasts emitted on May 17, 2014. (a) and (d) dressed deterministic forecasts, (b) and (e) Meteorological ensemble-based forecasts, (c) and (f) Meteorological ensemble+EnKF forecasts.

The utility function (eq. 4.6) is used successively with the five spending vectors presented in Table 4.2. The probabilities p_m with $m = 1...12$ in Eq. 4.6 correspond to the relative frequencies of each category after classification of forecast members that allows for computing the utility as a function of the money spent. The utility curve maximum provides the optimal spending associated with each forecast. Figure 4.8 illustrates an example for $A = 0.01$ and $\psi = 7$.
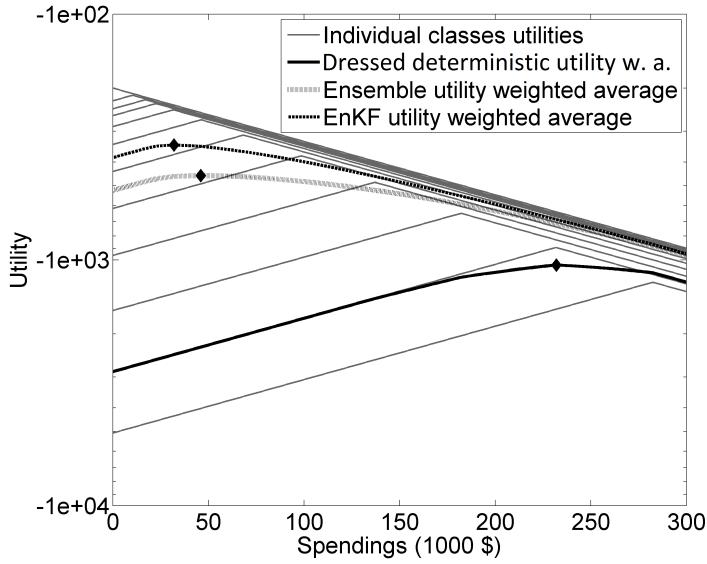
Figure 4.8: Utility as a function of money spent for forecasts emitted on May 17, 2014 for each of the three forecasting systems. Thin grey curves represent the utility of any decision given the 12 classes of events. Thick curves show the utility of forecasting system. Maxima of each system are indicated by a diamond marker. Calculations are for $A = 0.01$ and $\psi = 7$

Figure 4.9 presents the utility, hit rate and overspending as a function of parameter ψ for the three flood forecasting systems under study for various levels of risk aversion and for spending vector number 1 (see Table 4.2). Note that $A = 0$ corresponds to the case of a risk-neutral decision maker. Negative risk aversion values representing risk-seeking behaviour, were not used. As mentioned in section 4.6.2, any affine transformation of the utility function is admissible. In Figure 4.9, the utility of a perfect forecast was subtracted from the utility of each concurrent forecasting system and from the "no forecast" situation. This allows the y-axis of the utility plots to start at 0 and provide a common reference. This figure shows that a risk-neutral decision maker prefers having information from forecasts based on meteorological ensembles (with or without EnKF) rather than having no forecasts. However, for higher levels of risk aversion ($A = 0.01$, bottom line of Figure 4.9), the forecasting system has no usefulness for low levels of ψ.

60

Although this seems counter-intuitive, it can easily be explained by looking at the hydrographs (cf. Figure 4.4). Forecasts based on meteorological ensembles, in particular using EnKF, have a tendency to generate members with very high streamflow levels. As risk aversion increases, the decision maker puts more weight towards those members, as the associated damage is considerable. This causes the decision maker to spend large amounts of money to "insure" against the potential damage.

As such high streamflow levels are historically rare for the Montmorency River, the decision maker would have been better off not to spend any money and suffer damage during the relatively rare and comparatively small flood events. The "usual" flood events for the Montmorency River are not as dramatic as what is predicted by the most extreme scenarios of the predictive distribution. However, for a risk averse decision maker, large weights are attributed to those extreme scenarios. This encourages the decision maker to spend large amount of money to mitigate events that in fact never materialize.

Dressed deterministic forecasts decrease weakly with ψ, relative to the ensemble forecasts. Put differently, for large amounts of material damage, the dressed deterministic forecasts have much higher values than the ensemble forecasts. This is due to the fact that, for all lead times, ensemble forecasts include members having "unrealistic" streamflow values. This over-forecasting is exacerbated for high values of material damage and a high value of risk aversion. As the concavity of μ increases (due to an increase in the level of risk aversion A), "bad shocks" are weighted more heavily by the decision maker, leading to considerable levels of (over-) spending.
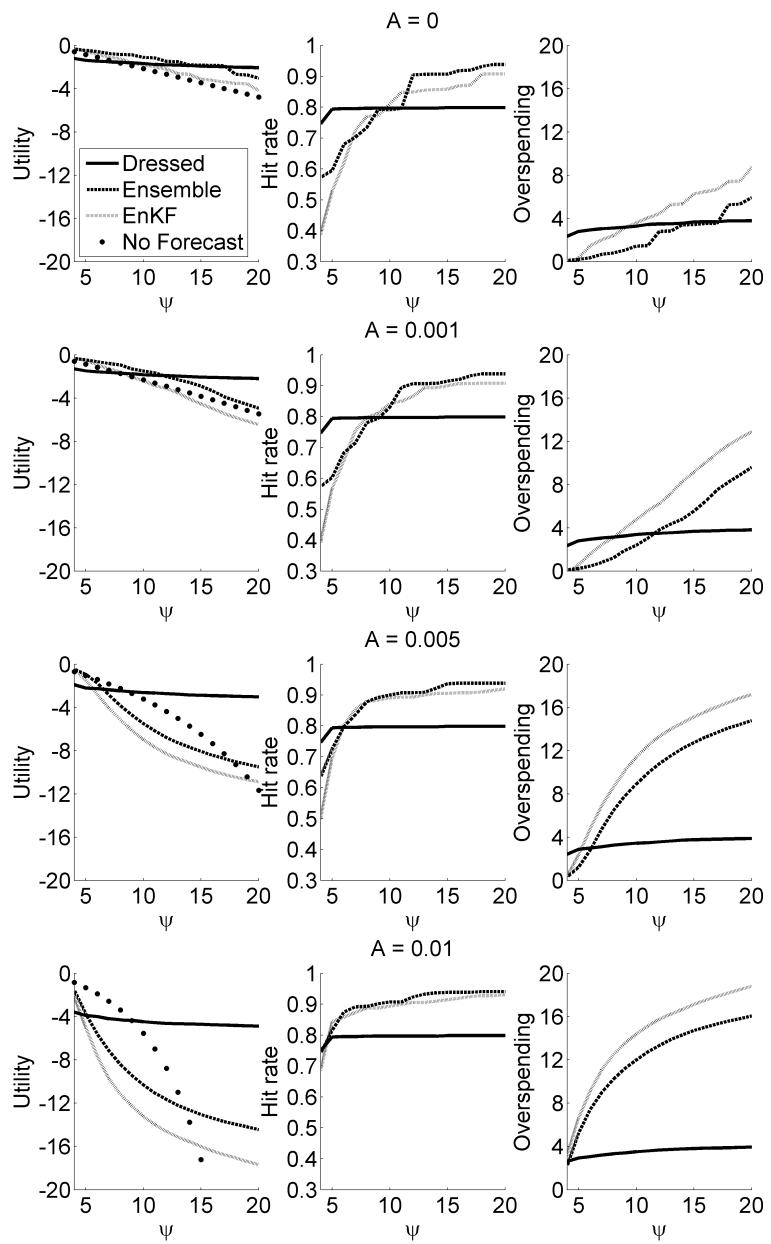
Figure 4.9: Utility, hit rate and overspending as a function of parameter ψ for the three flood forecasting systems for various levels of risk aversion for the decision maker, when spending is allowed indifferently at any lead time.

The same effect can be seen for alternative choices of spending vectors. Figure 4.10 shows the same parameters (utility, hit rate and overspending) as a function of ψ, for the same forecasts, but for spending vector number 2. With this spending vector, the decision maker cannot spend any amount of money five days ahead and can then progressively spend a greater percentage of the available money as the lead time decreases. In such a case, the decision maker should prefer to have access to forecasts based on meteorological ensembles (rather than the no forecast situation) if they are slightly risk-averse ($A = 0.001$). This is explained by the fact that the 5-day forecast (which contains extreme forecast members, c.f. Figure 4.4) is not used by the decision maker, which limits overspending.

Eventually, a more risk-averse decision maker ($A = 0.01$) should prefer the dressed forecasts over any other forecasting system, for ψ values over 6. This is again attributable mostly to some members of the ensemble systems frequently forecasting flood events that don't materialize. This is confirmed by the overspending graphs on the right-hand side of Figure 4.10. Hence, in Eq. 4.6, the optimal level of spending s is less for the dressed forecasts than for the other forecasting systems.

When ψ becomes very large (very important material damages) the utility of the "no forecast" framework decreases rapidly, especially for a more risk-averse decision maker. Then, even if the decision maker generally overspends, all forecasts are preferred to the "no forecast" situation since the damage associated with a flood event are considerable. For high values of ψ, the spending decision effectively acts as an (valuable) insurance policy. The hit rate increases (slightly) with the level of risk aversion. This is expected, as a risk-averse decision maker will attribute more importance to large streamflow values in the ensemble forecast.

The third column of Figure 4.10 shows that a risk-averse decision maker would reduce their overspending by using a forecasting system based on dressed deterministic forecasts rather than on meteorological ensemble forecasts with or without EnKF. Dressed deterministic forecasts exhibit much less dispersion than EnKF forecasts, which also accounts for state variable uncertainty. As it was remarked earlier, a risk-averse decision maker will put more weight on higher streamflow

values in the ensemble. If the spread is large, the ensemble necessarily includes larger streamflow values. It is therefore not surprising that overspending is larger for the ensemble forecast with the larger spread, especially for high values of both A and ψ.
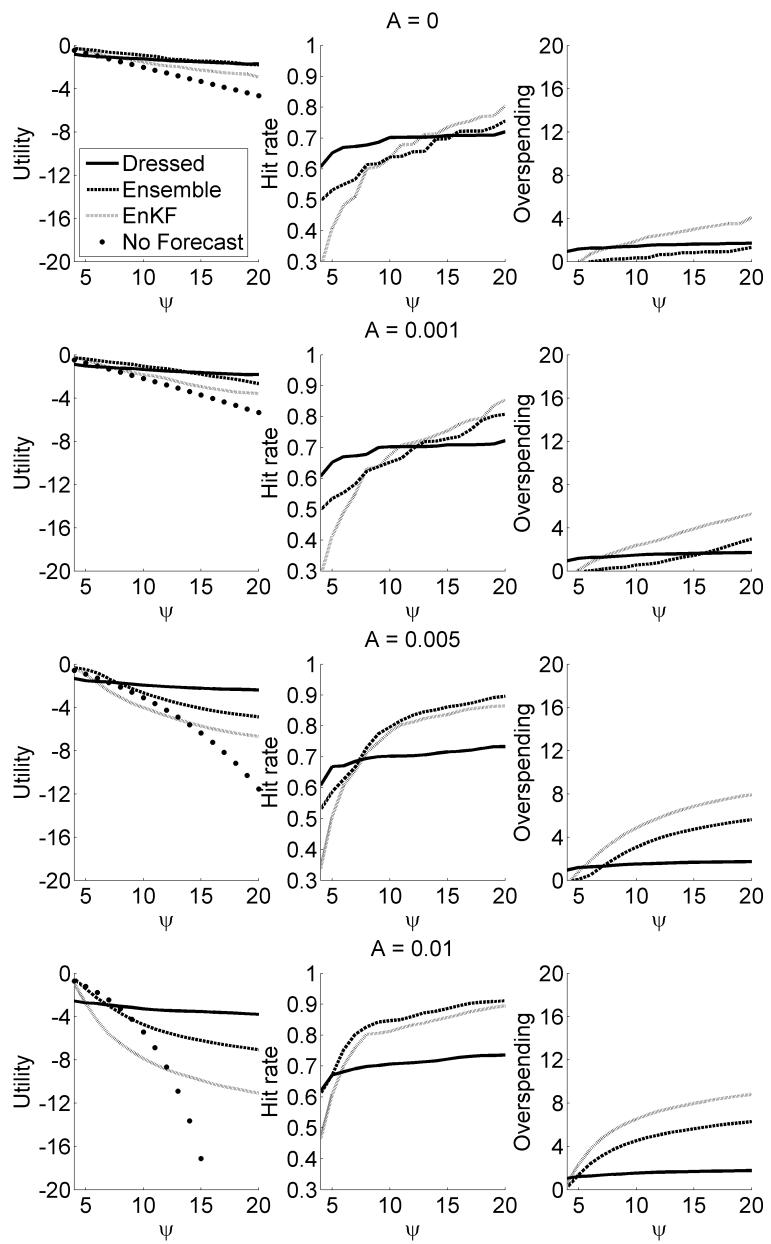
Figure 4.10: Utility, hit rate and overspending as a function of parameter ψ for the three flood forecasting systems for various levels of risk aversion by the decision maker, when the decision maker is allowed to spend an increasing fraction of the total available money as the lead time shortens.

65

The results for the other spending vectors (c.f. Table 4.2) are qualitatively similar and are therefore not presented. These results are available as supplementary material.

Figure 4.11 shows bar graphs of the relative frequency of each class of events, from 2 to 12, for the different forecasting systems and for observations (see section 4.7.2). The first class, which is the "no damages" class for low streamflow values, is not included. From this figure, it can be seen that all three systems forecast floods more frequently than they should (according to the observed frequencies). This over-forecasting also increases with the forecasting horizon. However, the frequencies computed from the dressed deterministic forecasts (panel a) are closer to the observed frequencies in each class. It can also be noted that the difference between forecasts based on meteorological ensembles without EnKF (b) and with EnKF (c) lies in the representation of extreme events at the 1-day lead time. There are more such over-forecasted situations at this lead time when the EnKF is used as part of the forecasting system. This is sufficient for the EnKF forecasts to have lower economic value than the forecasts relying only on meteorological ensembles.
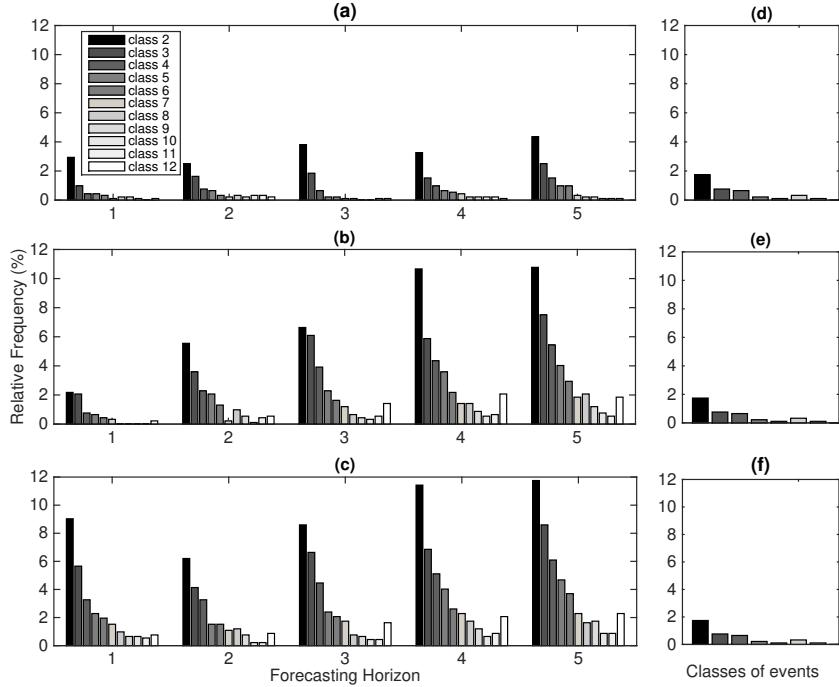
Figure 4.11: Relative frequencies of forecasts and observations corresponding to the classes of events used in the evaluation of damages, as a function of the forecasting horizon (1 to 5 days). (a) Dressed deterministic forecasts, forecasts based on meteorological ensembles without (b) and with (c) EnKF. Panels (d), (e) and (f) are identical and show the relative frequencies of the observations for the same classes.

4.8 Discussion

Throughout this paper, the impact of risk-aversion on the economic value of forecasts is assessed for a well-trained end-user. We find that risk-averse end-users mainly consider the less favorable scenarios (upper tail of the predictive distribution in the case of flood forecasting). Thus, although the members of the forecasts are truly equiprobable and presented as such to the end-user, they can still be weighted differently in his or her eyes. This is true for any level of risk aversion, but even more so for high levels of risk aversion. For example, Danhelka (2015) mentions:

The Minister simply asked me what the forecast for Prague was. After I have explained all the known information, forecasts and uncertainties, I gave him my best guess of the peak flow. But his response was: "No, no, no, give me the worst-case scenario; don't tell me numbers you cannot guarantee as not being exceeded".

Therefore, any 'outlier' leads to costly actions and the forecasts become of low or null economic value if these outliers are frequent. A consequence of this is that forecasters may be especially careful about the forecasts for high probability of non-exceedance.

The "real" level of risk aversion for the decision maker for flood emergency measures along the Montmorency River remains unknown due to the insufficient record of decisions and associated spending. However, it can be reasonably assumed that they are highly risk-averse (Claude Pigeon, personal communications). Considering $A = 0.01$ and Figure 4.10, the dressed deterministic forecasts provide maximal utility. They have a lower hit rate but also a much lower level of overspending compared to the other forecasting systems. This leads to the conclusion that dressed forecasts have the highest economic value for this level of risk aversion.

However, this conclusion relies on the assumption that benefits are linear. As the level of damage (i.e. $d(m)$) increases, so does the spending needed to alleviate this damage. In a situation where human casualties are possible (resulting in extremely high values of ψ), the spending needs not to increase with the value of the alleviated damages $d(m)$. For example, the cost of an evacuation is not linked to the (somewhat subjective) value associated with human casualties. These considerations are left for further research.

Our study also shows that forecast *quality* (as verified using metrics such as the CRPS) is not always a guarantee of forecast *value* in an economic sense. In this study, the streamflow forecasts based on meteorological ensembles have better CRPS than dressed deterministic forecasts, but their value according to the CARA utility function is lower.

In any case, it is capital to recall that the role of the forecaster is to issue the best possible streamflow forecast given their knowledge of the situation and available model and data. It is the

end-user's role to decide the course of action. In no way we would advocate for the forecasters to deliberately bias the forecasts for a certain user. Furthermore, in this paper we did not address the issue of potential cognitive biases and training issues for end-users, which is recognized in the literature (e.g Ramos et al., 2013; Demeritt et al., 2010; Doswell, 2004). The training of end-users and continuous interaction with forecasters should be encouraged to favor optimal decision-making.

Lastly, the decision-making process analyzed in this study is a static one. It would be even more realistic to analyse flood mitigation as a dynamic decision process. For instance, depending on their level of confidence regarding the 5-day forecast, a decision maker could decide to launch an evacuation alert and immediately spend all available funds for emergency measures. As stated in Roulin (2007), intuition lends to thinking that preparing in advance for a flood could lead to reduced overall spending compared with waiting until the last minute. This is also discussed in Morss (2010) in her analysis of three case studies of the interactions between flood forecasts, decisions and outcomes. She provides examples of the importance of early actions:

Key property- and life-saving decisions are often thought of as taking specific protective action immediately prior to or during an event. However, sometimes key decisions can be less evident and occur during earlier planning stages. For example, in Grand Forks, once officials had decided to expend most of their time, effort, and resources on planning and building primary dikes, they were not able to plan and build secondary dikes fast enough when the flood grew worse than expected. In the Pescadero case, if officials had not decided to position rescue crews and equipment before the flood began, they would not have been able to reach the area.

However, the implementation dynamic decision model also introduces many more questions regarding how the total spending should be distributed among lead times. It is thus left for further studies.

4.9 Conclusions

The purpose of this study is to set the basis of an alternative framework to replace the cost-loss ratio in economic assessment of early warning flood forecasting systems. This alternative framework is based on the Constant Absolute Risk Aversion (CARA) utility function which is well-known in economics. To the authors' knowledge, risk aversion is rarely, if ever, accounted for in hydro-economic assessment of flood warning systems. This new framework is used to compare the economic value of three concurrent streamflow ensemble forecasting systems using the flood-prone Montmorency River watershed in Quebec, Canada. This study concentrates on ensemble rather than deterministic forecasts, as the recent literature clearly states that ensemble forecasts are preferable to deterministic ones for numerous reasons (e.g. Krzysztofowicz, 2001; Jaun et al., 2008; Velazquez et al., 2010; He et al., 2013). Furthermore, real-life operations for the case study involved here (flood forecasting for the Montmorency River) do not involve deterministic forecasts. However, there exists many different means of constructing streamflow ensemble forecasts: dressed deterministic forecasts, single hydrological models fed with meteorological ensemble forecasts, multiple hydrological models, with or without data assimilation, etc. Those different forecasting systems can be compared in terms of their correspondence with the observation and in terms of their value for an end-user.

The importance of the level of risk aversion of the decision maker for the determination of the economic value of a streamflow forecasting system is illustrated by our results. A risk-neutral decision maker, as assumed in the cost-loss ratio framework, is rarely, if ever, encountered in real-life decision problems. The value of forecasting systems strongly depends on the decision maker's level of risk aversion and this parameter should be as much as possible targeted to the end-user. The results also show that forecast quality as assessed by the CRPS, or the reliability diagram, do not necessarily translate directly into a greater economic value, especially if the decision maker is not risk-neutral. Frequent over-forecasting strongly affects the economic value of forecasts. Over-

forecasting can be corrected by adequate statistical post-processing of the predictive distributions. This was judged outside of the scope of this study but could certainly be explored in further work. Adequate post-processing would likely improve the value of forecasts.

The decision-making framework presented here can be improved in some ways. Further studies could also include a more detailed, dynamic decision-making process, formally accounting for the forecast horizon. Furthermore, the decision maker could lose confidence in a "bad" forecasting system. The results presented in this paper implicitly assumed that the decision maker's trust of the forecast was absolute. Further studies could include an explicit description of the decision maker's learning about the reliability of a forecast.

4.10 Appendix A: How the cost-loss ratio implies risk-neutrality

Consider the simple case where the decision maker has two possible choices: $s = 0$ (no action) or $s = 1$ (action). The cost of implementing the action is denoted by $c > 0$. If the adverse event occur (e.g. flood), a damage of $d > 0$ is incurred. Let also b be the damage avoided if an action is taken by the decision maker (assuming $c < b \leq d$). Finally, let p be the probability of the adverse event.

Using the economic model presented in section 4.3, the vNM utility of the decision maker for each of the possible choices is:

$$U(s = 0) = p\mu(-d) + (1 - p)\mu(0) \tag{4.11}$$

$$U(s = 1) = p\mu(-d + b - c) + (1 - p)\mu(-c) \tag{4.12}$$

Straightforward algebra shows that an action is optimal (i.e. $U(s = 1) \geq U(s = 0)$) if, and only if,

$$p \geq \frac{\mu(0) - \mu(-c)}{\mu(0) - \mu(-c) + \mu(-d + b - c) - \mu(-d)} \tag{4.13}$$

If $\mu(\cdot)$ is concave (the decision maker is risk-averse), this is not equal to the cost-loss ratio. However, if the decision maker is risk-neutral, $\mu(\cdot)$ is linear, so for some $a_1 > 0$ and $a_2 \in \mathbb{R}$: $\mu(0) = a_2$, $\mu(-c) = -a_1 c + a_2$, $\mu(-d) = -a_1 d + a_2$ and $\mu(-d + b - c) = a_1(-d + b - c) + a_2$. Therefore, Eq. 4.13 reduces to:

$$p \geq \frac{c}{b} \tag{4.14}$$

If $b = d$ (all damages are avoided), this gives the usual cost-loss ratio.

Here, an important comment is in order. One could always define "cost" and "loss" as follows:

$$cost = \mu(0) - \mu(-c) \tag{4.15}$$

$$loss = \mu(0) - \mu(-c) + \mu(-d + b - c) - \mu(-d) \tag{4.16}$$

so an action is optimal if and only if:

$$p \geq \frac{cost}{loss} \tag{4.17}$$

However, this "black-box" analysis side-steps some interesting and important questions regarding the contribution of outcome versus risk preferences to the decision maker's utility. Using the vNM utility allows us to explicitly describe the impact of risk preferences on the value of forecasting systems. Note also that the hydrological literature (e.g. Roulin, 2007; Verkade and Werner, 2011; Muluye, 2011) almost always considers "cost" and "loss" to be defined in monetary units.

To see more clearly the impact of risk-aversion on the optimal decision, suppose that μ is CARA, i.e. $\mu(x) = \frac{-1}{A} \exp\{-Ax\}$, and that $b = d$. Using the formula above and straightforward algebra, we find that an action is optimal if

$$p \geq \frac{\exp\{Ac\} - 1}{\exp\{Ad\} - 1} \equiv t(A) \tag{4.18}$$

as opposed to $p \geq c/d$ for the cost-loss ratio. One can verify that $t(A)$ is strictly decreasing with $\lim_{A \to 0} t(A) = c/d$. Then, this implies that, as risk aversion increases, the decision maker requires lower confidence level (for the realisation of the adverse event) in order to take an action. The limiting case, when the decision maker is risk neutral, gives the cost-loss ratio.

4.11 Appendix B: Properties of the CARA utility function

We have: $\mu(x) = \frac{-1}{A}\exp\{-Ax\}$ for some real values for x and $A \neq 0$. One can easily verify that the first derivative with respect to x is: $\mu'(x) = \exp\{-Ax\} > 0$, and that the second derivative with respect to x is $-A\exp\{-Ax\}$. Therefore, μ is strictly concave if $A > 0$ and strictly convex if $A < 0$. Figure 4.1 illustrates a generic example for a CARA utility function.

The value of A reflects the decision maker's level of risk aversion. Specifically, the *Arrow-Pratt index of absolute risk aversion* is defined as

$$A(\mu) = \frac{-\mu''(\cdot)}{\mu'(\cdot)} \tag{4.19}$$

for all twice continuously differentiable function $\mu(\cdot)$. If $A(\mu) > A(\tilde{\mu})$, we say that the decision maker whose preferences are represented by μ is more risk-averse than a decision maker whose preferences are represented by $\tilde{\mu}$.

Using the parametric form: $\mu(x) = \frac{-1}{A}\exp\{-Ax\}$, we immediately see that $A(\mu) = A$. Since $A(\mu)$ is independent of x, we say that μ exhibits a constant absolute level of risk aversion.

Note that the CARA utility functions are only defined for $A \neq 0$. However, since an individual

is risk-neutral if and only if μ is linear, the utility function of any risk-neutral individual has the form $\mu(x) = a_1 x + a_2$ for $a_1 > 0$ and $a_2 \in \mathbb{R}$. In other words, there is no need to define a specific class of utility for risk-neutral individuals. As such, the CARA utility class needs only to apply to non-risk-neutral individuals.

The interested reader can consult chapter 2 in Gollier (2004), chapter 6 in Mas-Colell et al. (1995) or Levin (2006) for additional details.

4.12 Competing Interests

The authors declare that they have no conflict of interest.

4.13 Acknowledgements

Bibliography

Abaza, M., Anctil, F., Fortin, V., and Turcotte, R.: A comparison of the Canadian global and regional meteorological ensemble prediction systems for short-term hydrological forecasting, Monthly Weather Review, 142, 2561–2562, 2014.

Abaza, M., Anctil, F., Fortin, V., and Turcotte, R.: Exploration of sequential streamflow assimilation in snow dominated watersheds, Advances in Water Resources, 80, 79–89, 2015.

Babcock, B. A., Choi, E. K., and Feinerman, E.: Risk and probability premiums for CARA utility functions, Journal of Agricultural and Resource Economics, pp. 17–24, 1993.

Beven, K.: Facets of uncertainty: epistemic uncertainty, non- stationarity, likelihood, hypothesis testing, and communication, Hydrological Sciences Journal, 61, 1652–1665, 2016.

Bisson, J.-L. and Roberge, F.: Prévisions des apports naturels: Expérience d'Hydro-Québec, Atelier sur la prévision du débit, Toronto, 1983.

Boucher, M.-A., Tremblay, D., Delorme, L., Perreault, L., and Anctil, F.: Hydro-economic assessment of hydrological forecasting systems, Journal of Hydrology, 416—417, 133–144, 2012.

Carpentier, P.-L., Gendreau, M., and Bastien, F.: Long-term management of a hydroelectric multireservoir system under uncertainty using the progressive hedging algorithm, Water Resources Research, 49, 2812–2827, 2013.

Carsell, K., Pingel, N., and Ford, D.: Quantifying the benefit of a flood warning system, Natural Hazard Review, 5, 131–140, 2004.

Cerdá Tena, E. and Quiroga Gómez, S.: Cost-Loss Decision Models with Risk Aversion, 01, Instituto Complutense de Estudios Internacionales, 2008.

Côte, P. and Leconte, R.: Comparison of stochastic optimization algorithms for hydropower reservoir operation with ensemble streamflow prediction, Journal of Water Resources Planning and Management, 142, doi:10.1061/(ASCE)WR.1943-5452.0000575, 2016.

Danhelka, J.: On decisions under uncertainty, `http://hepex.irstea.fr/on-decisions-under-uncertainty/`, published online: 2015-05-01, 2015.

Demeritt, D., Nobert, S., Cloke, H., and Pappenberger, F.: Challenges in communicating and using ensembles in operational flood forecasting, Meteorological Applications, 17, 209–222, 2010.

Doswell, C.: Weather forecasting by Humans - Heuristics and Decision Making, Weather and Forecasting, 19, 1115–1126, 2004.

Duan, Q., Sorroshian, S., and Gupta, V.: Optimal use of the SCE-UA global optimization method for calibrating watershed models, Journal of Hydrology, 158, 265–284, 1994.

Evensen, G.: The Ensemble Kalman Filter: theoretical formulation and practical implementation, Ocean Dynamics, 53, 343–367, 2003.

Fishburn, P.: Retrospective on the Utility Theory of von Neumann and Morgenstern, Journal of Risk and Uncertainty, 2, 127–158, 1989.

Fortin, J.-P., Moussa, R., Bocquillon, C., and Villeneuve, J.-P.: HYDROTEL, un modèle hydrologique distribué pouvant bénéficier des données fournies par la télédétection et les systèmes d'information géographique, Revue des Sciences de l'Eau / Journal of Water Science, 8(1), 97–124, 1995.

Fortin, V.: Le modèle météo-apport HSAMI : historique, théorie et application, Rapport de recherche (Révision 1.5), Tech. rep., Institut de Recherche d'Hydro-Québec, 2000.

Franz, K. and Ajami, N.: Hydrologic ensemble prediction experiment focuses on reliable forecasts, Eos, 86, 239, 2005.

Gollier, C.: The economics of risk and time, MIT Press, 2004.

Gompertz, B.: On the Nature of the Function Expressive of the Law of Human Mortality, and on a New Mode of Determining the Value of Life Contingencies, Philosophical Transactions of the Royal Society of London, 115, 513–583, 1825.

He, Y., Wetterhall, F., Cloke, H., Pappenberger, F., Wilson, M., Freer, J., and McGregor, G.: Tracking the uncertainty in flood alerts driven by grand ensemble weather predictions, Meteorological Applications, 16, 91–101, 2013.

Huard, D.: Analyse et intégration d'un degré de confiance aux prévisions de débits en rivière, Tech. rep., David Huard Solution, Quebec, 2013.

Jaun, S., Ahrens, B., Walser, A., Ewen, T., and Schar, C.: A probabilistic view on the August 2005 floods in the upper Rhine catchment, Natural Hazard and Earth System Sciences, 8, 281–291, 2008.

Juston, J., Kauffeldt, A., Montano, B., Seibert, J., Beven, K., and Westerberg, I.: Smiling in the rain: Seven reasons to be positive about uncertainty in hydrological modelling, Hydrological Processes, 27, 1117–1122, 2013.

Katz, R. and Murphy, A.: Economic value of weather and climate forecasts, Cambridge University Press, New York, 1997.

Krzysztofowicz, R.: Expected utility, benefit, and loss criteria for seasonal water supply planning, Water Resources Research, 22, 303–312, 1986.

Krzysztofowicz, R.: The case for probabilistic forecasting in hydrology, Journal of Hydrology, 249, 2–9, 2001.

Lave, T. and Lave, L.: Public perception of the risks of floods: Implications for communication, Risk Analysis, 11, 255–267, 1991.

Leclerc, M. and Secretan, Y.: Reconstruction de la prise d'eau de l'Arrondissement Charlesbourg – Simulation hydrodynamique du secteur Canteloup, des Îlets, Trois-Saults de la rivière Montmorency, Tech. Rep. R1416, INRS-Eau and Laval University, Quebec, 2012.

Leclerc, M., Morse, M., Francoeur, J., Heniche, M., Boudreau, P., and Secretan, Y.: Analyse de risques d'inondations par embâcles de la rivière Montmorency et identification de solutions techniques innovatrices – Rapport de la Phase I – Préfaisabilité, Tech. Rep. R577, INRS-Eau and Laval University, Quebec, 2001.

Levin, J.: Choice under uncertainty, Lecture Notes, URL `http://web.stanford.edu/\%7Ejdlevin/Econ\%20202/Uncertainty.pdf`, 2006.

Lighthill, M. and Whitham, G.: On kinematic waves, I. Flood movement in long rivers, Proceedings of the Royal Society, Series A, 229, 281–316, 1955.

Mamono, A.: Mise à jour des variables d'état du modèle hydrologique HYDROTEL en fonction des débits mesurés, Master's thesis, Université du Québec à Montréal, 2010.

Mandel, J.: Efficient implementation of the Ensemble Kalman Filter, Tech. Rep. R1416, University of Colorado at Denver and Health Sciences Center, Denver, 2006.

Mas-Colell, A., Whinston, M. D., and Green, Jerry, R.: Microeconomic theory, vol. 1, Oxford University Press New York, 1995.

Matheson, J. E. and Winkler, R. L.: Scoring rules for continuous probability distributions, Management Science, 22, 1087–1096, 1976.

Merz, B., Elmer, F., and Thieken, A.: Significance of "high probability/low damage" versus "low probability/high damage" flood events, Natural Hazards and Earth System Sciences, 9, 1033–1046, 2009.

Morss, R.: Interactions among flood predictions, decisions, and outcomes: Synthesis of three cases, Natural Hazards Review, 11, 83–96, 2010.

Muluye, G.: Implications of medium-range numerical weather model output in hydrologic applications: Assessment of skill and economic value, Journal of Hydrology, 400, 448–464, 2011.

Murphy, A.: The value of climatological, categorical and probabilistic forecasts in the cost-loss ratio situation, Monthly Weather Review, 105, 803–816, 1977.

Pope, R. and Just, R.: On testing the structure of risk preferences in agricultural supply analysis, Agricultural Journal of Agricultural Economics, 73, 743–748, 1991.

Ramos, M.-H., van Andel, S., and Pappenberger, F.: Do probabilistic forecasts lead to better decisions?, Hydrology and Earth System Sciences, 17, 2219–2232, 2013.

Richardson, D.: Skill and relative economic value of the ECMWF ensemble prediction system, Quarterly Journal of the Royal Meteorological Society, 126, 649–667, 2000.

Rothschild, M. and Stiglitz, J. E.: Increasing risk: I. A definition, Journal of Economic theory, 2, 225–243, 1970.

Roulin, E.: Skill and relative economic value of medium-range hydrological ensemble predictions, Hydrology and Earth System Sciences, 11, 725–737, 2007.

Rousseau, A., Savary, S., and Konan, B.: Implantation du modèle HYDROTEL sur le bassin de la rivière Montmorency afin de simuler les débits observés et de produire des scénarios de crues du printemps pour l'année 2008, Tech. Rep. R921, INRS-Eau, Quebec, 2008.

Schaake, J. C., Hamill, T. M., Buizza, R., and Clark, M.: The hydrological ensemble prediction experiment, Bulletin of the American Meteorological Society, 88, 1541, 2007.

Shorr, B.: The cost/loss utility ratio, Journal of Applied Meteorology, 5, 801–803, 1966.

Stanski, H., Wilson, L., and Burrows, W.: Survey of common verification methods in meteorology, Tech. Rep. World Weather Watch Technical Report No. 8, WMO/TD No.358, David Huard Solution, Geneva, 1989.

Thiboult, A. and Anctil, F.: On the difficulty to optimally implement the Ensemble Kalman filter: An experiment based on many hydrological models and catchments, Journal of Hydrology, 529, 1147–1160, 2015.

Thiboult, A., Anctil, F., and Boucher, M.-A.: Accounting for three sources of uncertainty in ensemble hydrological forecasting, Hydrology and Earth System Science, 20, doi:10.5194/hess-20-1809-2016, 2016.

Turcotte, B. and Morse, B.: River ice breakup forecast and annual risk distribution in a climate change perspective, in: 18th Workshop on the Hydraulics of Ice Covered Rivers, CGU HS Committee on River Ice Processes and the Environment, Quebec, 2015.

US Army Corps of Engineers: Framework for estimating national economic development benefits and other beneficial effects of flood warning and preparedness systems., Tech. Rep. 94-R-3, US Army Corps of Engineers, Alexandria, Virginia, USA, 1994.

Van Dantzig, D. and Kriens, J.: Het economisch beslissingsprobleem inzake de beveiliging van Nederland tegen stormvloeden, pp. 157–170, Maris, A., De Blocq van Kuffeler, V., Harmsen, W., Jansen, P., Nijhoff, G., Thijsse, J., Verloren van Themaat, R., De Vries, J., Van der Wal, L. (Eds.), 1960.

Velazquez, J., Anctil, F., and Perrin, C.: Performance and reliability of multimodel hydrological ensemble simulations based on seventeen lumped models and a thousand catchments, Hydrology and Earth System Sciences, 14, 2303–2317, 2010.

Verkade, J. and Werner, G.: Estimating the benefits of single value and probability forecasting for flood warning, Hydrology and Earth System Sciences, 15, 3751–3765, 2011.

von Neumann, J. and Morgenstern, O.: Theory of games and economic behavior, vol. 60, Princeton University Press Princeton, 1944.

Werner, J.: risk aversion, in: The New Palgrave Dictionary of Economics, edited by Durlauf, S. N. and Blume, L. E., Palgrave Macmillan, Basingstoke, 2008.

Zhu, Y., Toth, Z., Wobus, R., and Mylne, K.: The economic value of ensemble-based weather forecasts, Bulletin of the American Meteorological Society, 83, 73–83, 2002.

5. Synthèse et conclusion

Les objectifs de ce projet étaient de comparer différentes approches de modélisation hydrologique et de construire une plateforme de comparaison des performances basée sur l'analyse de la valeur économique.

Le projet conclut que les prévisions hydrologiques conçues à partir de l'incertitude météorologique et tenant compte de la variabilité de l'état initial du bassin performent le mieux selon des critères de fiabilité et de résolution. En soit, cette conclusion n'est ni novatrice, ni utile à la plupart des utilisateurs des prévisions. Pour que ceux-ci soient prêts à transiger vers un nouveau système prévisionnel, une preuve de leur utilité justifiant un changement est plus complexe à apporter.

Le deuxième objectif de ce projet visait à répondre à cette exigence. Un outil de mesure de la valeur économique de la prévision hydrologique a été développé. Celui-ci se base sur l'utilité de la prévision dans un contexte d'application de prévention des inondations. Des facteurs comme la valeur intangible de la sécurité humaine et l'aversion au risque de preneur de décision ont été montrés comme étant à la fois indispensable à l'analyse, et ayant un fort impact sur les résultats.

Les résultats démontrent qu'un système de prévision performant le mieux selon les mesures standards (CRPS, fiabilité) ne va pas pour autant apporter une valeur économique accrue dans les mains du décideur. Il est également démontré que la

fiabilité de la partie supérieure de l'ensemble de prévision (forts débits peu probables) a un impact majeur sur la valeur de la prévision. En ce sens, la prévision dite « habillée » semble être la meilleure option dans la plupart des scénarios, vu la qualité conservatrice de la partie supérieure de la prévision.

Le système d'analyse économique développé dans ce projet n'est pas sans lacunes. Il a pour intention d'offrir une nouvelle approche et encourager des travaux futurs pour l'analyse de la valeur des prévisions hydrologiques en se distançant de l'analyse simpliste de ratio coût-perte, qui était jusque-là un outil populaire pour cette application. L'approche multidisciplinaire (en partenariat avec la discipline de l'économie) utilisée dans le développement de la méthode du projet se veut comme un encouragement à travailler de concert avec un secteur académique qui a beaucoup à nous apprendre sur les modèles de décision en présence d'incertitude. Ceci devient possible et plus intéressant maintenant que les prévisions probabilistes sont au premier rang de la discipline hydrologique.

Ce projet ouvre plusieurs portes sur des travaux futurs. Plusieurs aspects ayant été omis de la méthode actuelle pourraient être développés : un modèle de décision dynamique qui se « souvient » des décisions antérieures ou un utilisateur dont la confiance envers le système n'est pas absolue et dépend de la réussite des prévisions précédentes, ne sont que quelques exemples.

Aussi, il est à mentionner que bien que les embâcles soient au cœur de la problématique d'inondations sur la Montmorency, ceux-ci ne sont pas simulés par le modèle de prévision (opérationnel, ou suggéré). Cette lacune offre une piste d'amélioration grandement méritée au travail actuel.

Références

Abaza, M., Anctil, F., Fortin, V., and Turcotte, R.: A comparison of the Canadian global and regional meteorological ensemble prediction systems for short-term hydrological forecasting, Monthly Weather Review, 142, 2561–2562, 2014.

Abaza, M., Anctil, F., Fortin, V., Turotte, R. Exploration of sequential Streamflow assimilation in snow dominated watersheds. Advances in water resources, 80 (2015) 78-89.

Boucher, M. A., Tremblay, D., Delorme, L., Perreault, L., & Anctil, F. Hydro-economic assessment of hydrological forecasting systems. Journal of Hydrology, 416–417(0), 133-144. 2012

Boucher, M.-A., Tremblay, D., Delorme, L., Perreault, L., and Anctil, F.: Hydro-economic assessment of hydrological forecasting systems, Journal of Hydrology, 416—417, 133–144, 2012.

Brier, G. W., "Verification of Forecasts Expressed in Terms of Probability," Monthly Weather Review, 78, 1–3. 1950.

Carpentier, P.-L., Gendreau, M., and Bastien, F.: Long-term management of a hydroelectric multireservoir system under uncertainty using the progressive hedging algorithm, Water Resources Research, 49, 2812–2827, 2013.

Côte, P. and Leconte, R.: Comparison of stochastic optimization algorithms for hydropower reservoir operation with ensemble streamflow prediction, Journal of Water Resources Planning and Management, 142, doi:10.1061/(ASCE)WR.1943-5452.0000575, 2016.

Diomede, T., Nerozzi, F., Paccagnella, T., and Todini, E.: The use of meteorological analogues to account for LAM QPF uncertainty, Hydrology and Earth System Science, 12, 141–157, 2008.

Evensen G. The ensemble Kalman filter: theoretical formulation and practical implementation. Ocean Dynamics 53(4): 343–367. 2003.

Fortin, J.-P., Moussa, R., Bocquillon, C., and Villeneuve, J.-P.: HYDROTEL, un modèle hydrologique distribué pouvant bénéficier des données fournies par la télédétection et les systèmes d'information géographique, Revue des Sciences de l'Eau / Journal of Water Science, 8(1), 97–124, 1995.

Gneiting, T., & Raftery, A. E. Strictly Proper Scoring Rules, Prediction, and Estimation. Journal of the American Statistical Association, 102(477), 359-378. (2007)

Gouvernement du Québec. Le Québec chiffres en main – Édition 2014. Institut de la statistique du Québec, 72 p. [En ligne]. [http://www.stat.gouv.qc.ca/quebec-chiffre-main/pdf/qcm2014_fr.pdf]

Gouvernement du Québec. Ministère du développement durable et de la Lutte contre les Changements Climatique 2014 [En ligne]

Hamill, T. and Whitaker, J.: Probabilistic quantitative precipitation forecasts based on reforecast analogs: Theory and application, Monthly Weather Review, 134, 3209–3229, 2006.

He, Y.,Wetterhall, F., Cloke, H., Pappenberger, F.,Wilson, M., Freer, J., and McGregor, G.: Tracking the uncertainty in flood alerts driven by grand ensemble weather predictions, Meteorological Applications, 16, 91–101, 2013.

Huard, D.: Analyse et intégration d'un degré de confiance aux prévisions de débits en rivière, Tech. rep., David Huard Solution, Quebec, 2013.

Jaun, S., Ahrens, B., Walser, A., Ewen, T., and Schar, C.: A probabilistic view on the August 2005 floods in the upper Rhine catchment, Natural Hazard and Earth System Sciences, 8, 281–291, 2008.

Leclerc, M. and Secretan, Y.: Reconstruction de la prise d'eau de l'Arrondissement Charlesbourg – Simulation hydrodynamique du secteur Canteloup, des Îlets, Trois-Saults de la rivière Montmorency, Tech. Rep. R1416, INRS-Eau and Laval University, Quebec, 2012.

Mamono, Albe. Mise à jour des variables d'état du modèle hydrologique HYDROTEL en fonction des débits mesurés (mémoire de maitrise). Université du Québec à Montréeal, 66 pages. 2010

Marty, R., Zin, I., Obled, C., Bontron, G., and Djerboua, A.: Toward real-Time daily PQPF by an analog sorting approach: application to flash-flood catchments, Journal of Applied Meteorology and Climatology, 51, 505–520, 2012.

Murphy, A. H., What is a good forecast? An essay on the nature of goodness in weather forecasting, Weather Forecast., 8(2),281–293. 1993

Murphy, A.: The value of climatological, categorical and probabilistic forecasts in the cost-loss ratio situation, Monthly Weather Review, 105, 803–816, 1977.

OBV Charlevoix-Montmorency. Plan directeur de l'eau de la zone hydrique Charlevoix-Montmorency. Chapitre 2. Bassin versant de la rivière Montmorency. Présenté au ministère du Développement durable, de l'Environnement et de la Lutte contre les changements climatiques. Août 2014. 903 pages.

Richardson, D.: Skill and relative economic value of the ECMWF ensemble prediction system, Quarterly Journal of the Royal Meteorological Society, 126, 649–667, 2000.

Roulin, E.: Skill and relative economic value of medium-range hydrological ensemble predictions, Hydrology and Earth System Sciences, 11, 725–737, 2007.

Velazquez, J., Anctil, F., and Perrin, C.: Performance and reliability of multimodel hydrological ensemble simulations based on seventeen lumped models and a thousand catchments, Hydrology and Earth System Sciences, 14, 2303–2317, 2010.

Verkade, J. and Werner, G.: Estimating the benefits of single value and probability forecasting for flood warning, Hydrology and Earth System Sciences, 15, 3751–3765, 2011.

von Neumann, J. and Morgenstern, O.: Theory of games and economic behavior, vol. 60, Princeton University Press Princeton, 1944.

Annexe A

Résultats complémentaires

Les figures qui suivent ont été omises de l'article à des fins de breveté, et sont

offerte comme matériel supplémentaire.

La figure A-1 montre la sensibilité des paramètres Beta et d'aversion au risque en

appliquant différentes valeurs au processus de décision touchant à la prévision du 17

mai 2014. Les figures A-2 et A-3 montrent l'analyse d'autres limitations de dépenses

suite à la prévision, et leurs impacts sur l'utilité de la décision.
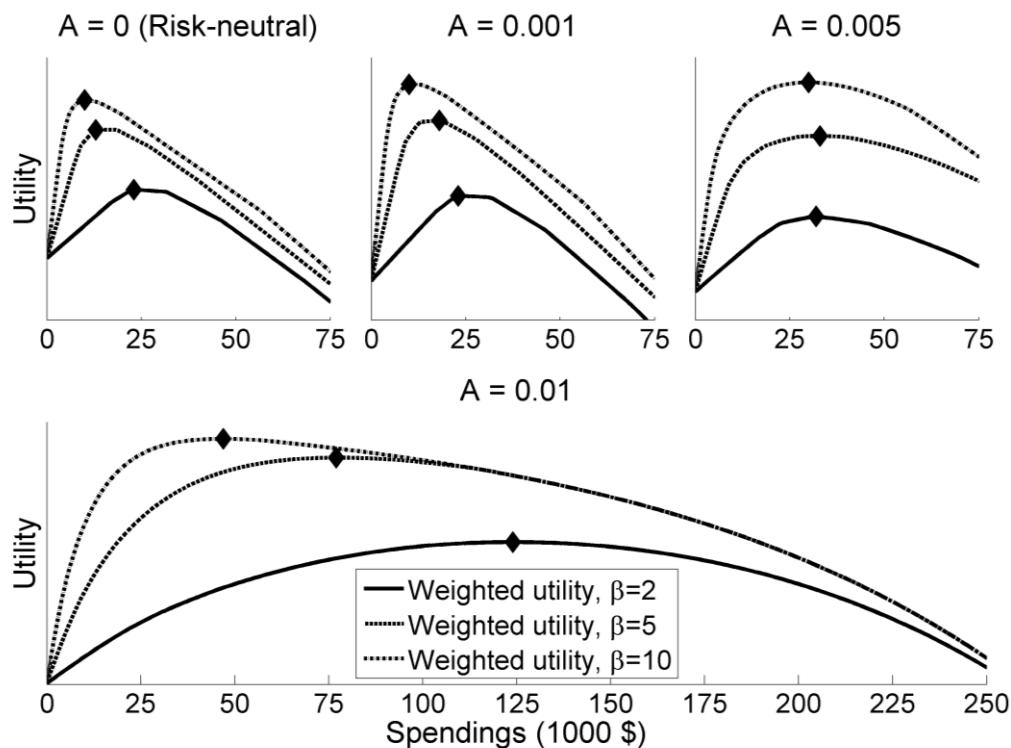
Figure A-1 - Utilité en fonction de l'argent dépensé pour les prévisions émises le 17 mai 2014, et ce pour le système de prévision EnKF. L'utilité optimale (identifiée par un marqueur losange) se déplace en fonction du paramètre Beta et du niveau d'aversion au risque.
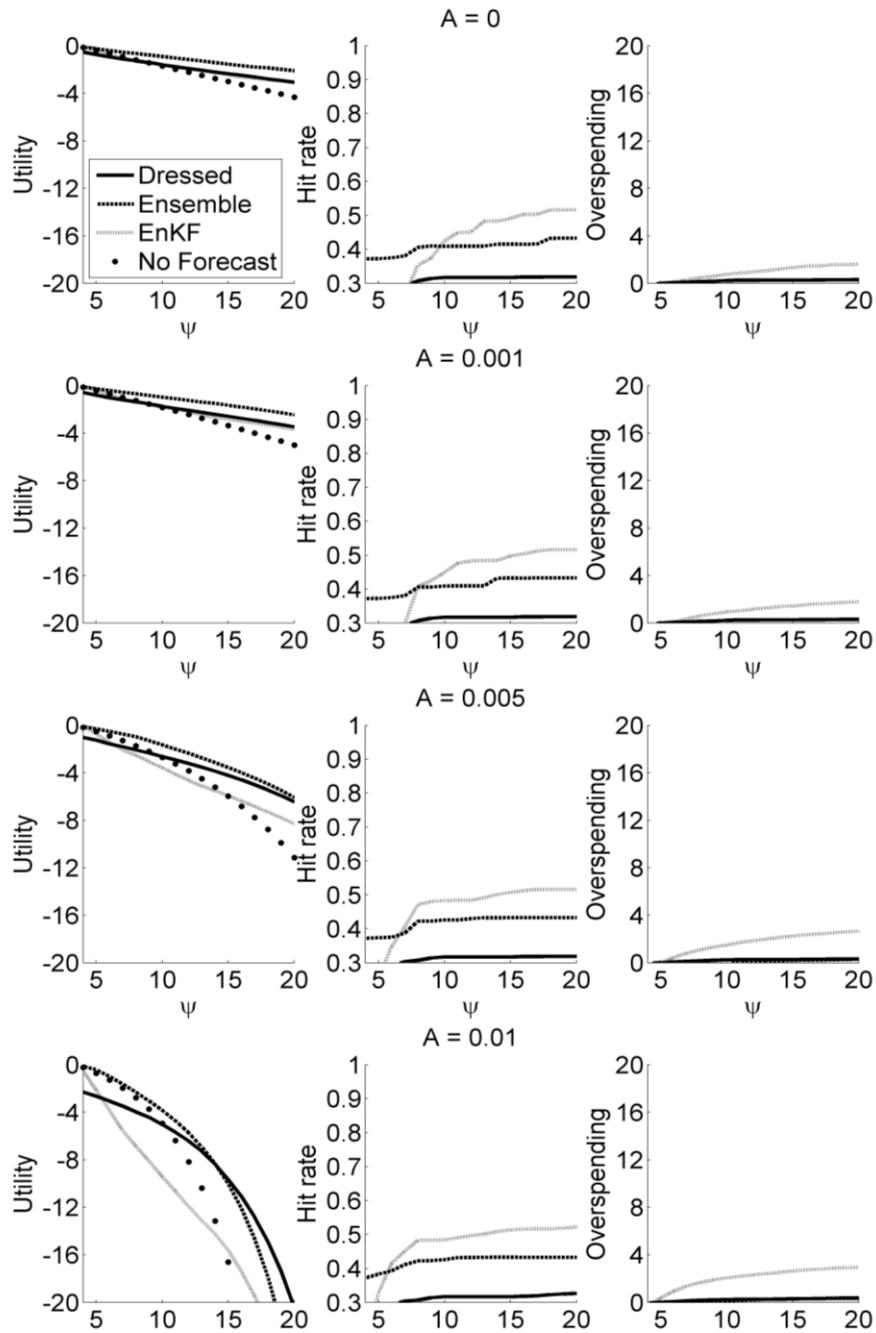
Figure A-2- Utilité, évènements détectés et sur-dépenses en fonction du paramètre ψ pour les trois systèmes de prévisions et pour différentes valeur d'aversion au risque de l'utilisateur, lorsque les dépenses ne sont possibles que lors de la dernière journée (journée de l'évènement)
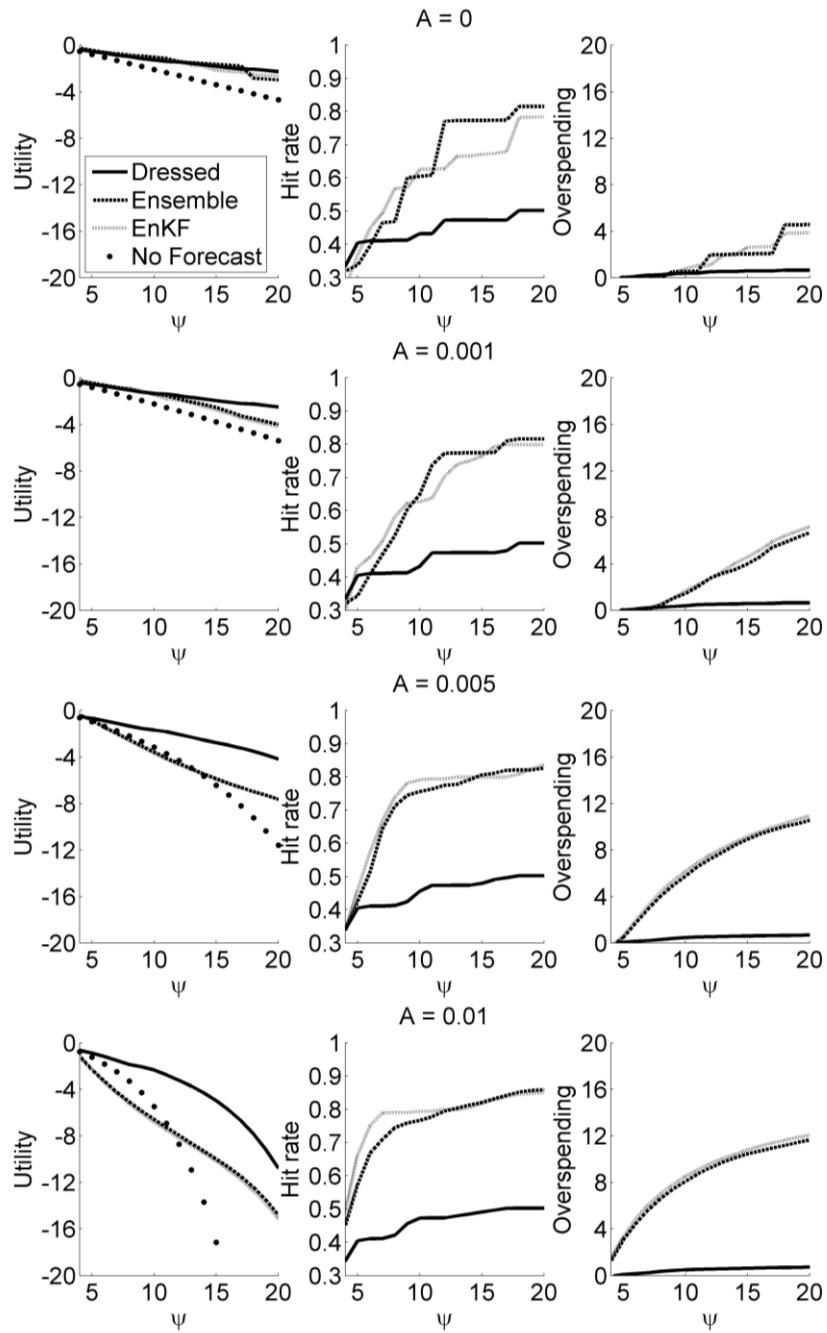
Figure A-3- Utilité, évènements détectés et sur-dépenses en fonction du paramètre ψ pour les trois systèmes de prévisions et pour différentes valeur d'aversion au risque de l'utilisateur, lorsque les dépenses sont permises de façon chronologiquement décroissante à mesure que l'évènement approche.